X-ray Constraints on Sterile Neutrinos + General Phase Space Density Constraints on the DM Particle

Casey R. Watson
Millikin University
July 25, 2013

Many Thanks to
My Collaborators:
Zhiyuan Li (CfA/UCLA) & Joe Cheeney, Chris Pelikan, Nick Polley, Leon Yu (Millikin)
and
Hector J. de Vega & Norma Sanchez
for inviting me.

OUTLINE

- **Properties of Sterile Neutrinos**
- **Models of Sterile Neutrino Interactions & Production**
- **X-ray Constraints from Previous Studies**
  - **CXB**
  - **Galaxy Clusters**
  - **Dwarf Galaxies**
- **The Advantages of Andromeda**
- **Constraints from *XMM* Observations of Andromeda**
- **Constraints from *Chandra* Observations of Andromeda**
- **The Road to Improved Constraints**
  - **Issues with Current-Generation Detectors**
  - **Expectations for Next-Generation Detectors**
- **Generalized Phase Space Density Constraints**
- **Summary & Conclusion**

The Fertile Phenomenology of Sterile Neutrinos

- **Non-zero active neutrino masses [1,2]**
- **Baryon & Lepton Asymmetries [15-20]**
- **Big Bang Nucleosynthesis [19]**
- **Evolution of the matter power spectrum [21,22]**
- **Reionization [23-31]**
- **Active Neutrino Oscillations [32-33]**
- **Pulsar Kicks [34-39]**
- **Supernovae [40-42]**
- **Excellent Dark Matter Particle Candidate [3-14, 43-57]**
- ***Most Importantly: Readily Testable***
  - ***Can decay into detectable X-ray photons***

Detecting Sterile Neutrino Radiative Decays:

$$\text{“}\nu_s\text{”} \rightarrow \text{“}\nu_\alpha\text{”} + \gamma$$

$$E_\gamma = \frac{m_s}{2} \sim 1 \text{ keV}$$

If

1 keV < m_s < 20 keV, *Chandra* & XMM can detect the X-ray photons associated with sterile neutrino radiative decays.

Sterile Neutrino Interactions with SM Particles

(Abazajian, Fuller, Patel 2001 [5]; Abazajian, Fuller, Tucker 2001 [6])

Very small mixing $(\sin^2 2\theta \lesssim 10^{-7})$ between

mass $|\nu_{1,2}>$ &

flavor $|\nu_{\alpha,s}>$ states:

$$|\nu_\alpha\rangle = \cos\theta|\nu_1\rangle + \sin\theta|\nu_2\rangle$$
$$|\nu_s\rangle = -\sin\theta|\nu_1\rangle + \cos\theta|\nu_2\rangle$$

For $m_s < m_e$,

3ν Decay Mode Dominates:

$$\Gamma_{3\nu} \simeq 1.74\times 10^{-30}s^{-1}\left(\frac{\sin^2 2\theta}{10^{-10}}\right)\left(\frac{m_s}{\text{keV}}\right)^5$$

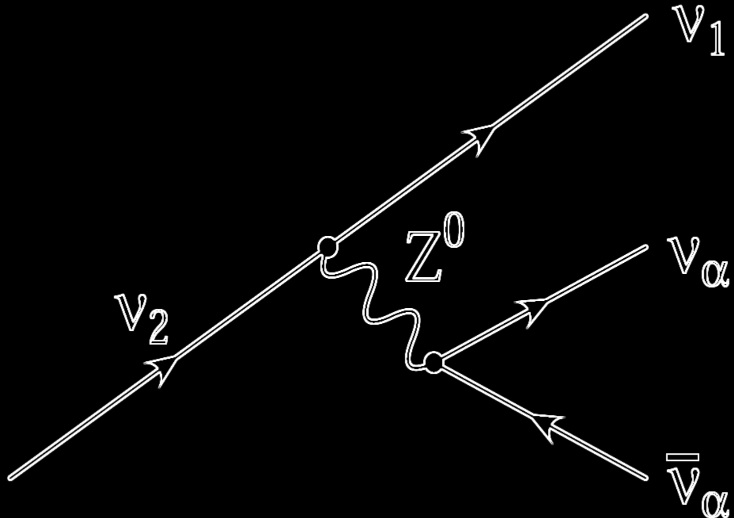

Radiative Decay Rate is:

$$\Gamma_s \simeq 1.36\times 10^{-32}s^{-1}\left(\frac{\sin^2 2\theta}{10^{-10}}\right)\left(\frac{m_s}{\text{keV}}\right)^5 \quad \nu_s \longrightarrow \nu_\alpha + \gamma$$

The Sterile Neutrino Radiative Decay Signal:

- Radiative Decay Luminosity:

$$\mathrm{L}_{\mathrm{x,s}} = E_{\gamma,s} N_s^{FOV} \Gamma_s = \frac{m_s}{2}\left(\frac{M_{DM}^{FOV}}{m_s}\right)\Gamma_s$$

$$\simeq 1.2 \times 10^{33} \mathrm{erg}\ s^{-1} \left(\frac{M_{DM}^{FOV}}{10^{11} M_\odot}\right) * \left(\frac{\sin^2 2\theta}{10^{-10}}\right)\left(\frac{m_s}{\mathrm{keV}}\right)^5$$

- Measured Flux: $\Phi_{x,s} = \frac{\mathrm{L}_{x,s}}{4\pi D^2}$

$$\phi_{x,s}(\sin^2 2\theta) \simeq 1 \times 10^{-17} \mathrm{erg\ cm}^{-2} s^{-1} \left(\frac{D}{\mathrm{Mpc}}\right)^{-2}$$

$$\times \left(\frac{M_{DM}^{FOV}}{10^{11} M_\odot}\right)\left(\frac{\sin^2 2\theta}{10^{-10}}\right)\left(\frac{m_s}{\mathrm{keV}}\right)^5$$

Sterile Neutrino Production:

- Dodelson-Widrow Model [3]
  - Density-Production Relationship [43]:

$$\mathbf{m_s = 55.5\ keV} \left(\frac{\sin^2 2\theta}{10^{-10}}\right)^{-0.615} \left(\frac{\Omega_s}{0.24}\right)^{0.5}$$

(for T_{QCD} ~ 170 MeV)

  - Mixing Angle-Independent Flux:

$$\phi_{x,s}(\Omega_s) \simeq 7.0 \times 10^{-15} \mathrm{erg\ cm^{-2}} s^{-1} \left(\frac{D}{\mathrm{Mpc}}\right)^{-2} \times \left(\frac{M_{DM}^{FOV}}{10^{11} M_\odot}\right) \left(\frac{\Omega_s}{0.24}\right)^{0.813} \left(\frac{m_s}{\mathrm{keV}}\right)^{3.374}$$

  - Agrees with Asaka et al. model [48] for

$$\mathbf{1\ keV \lesssim m_s \lesssim 10\ keV}$$

To maximize the sterile neutrino decay signal:

$$\phi_{x,s}(\sin^2 2\theta) \simeq 1.0 \times 10^{-17} \mathrm{erg\ cm^{-2} s^{-1}} \left(\frac{D}{\mathrm{Mpc}}\right)^{-2} \times \left(\frac{M_{DM}^{FOV}}{10^{11} M_\odot}\right) \left(\frac{\sin^2 2\theta}{10^{-10}}\right) \left(\frac{m_s}{\mathrm{keV}}\right)^{5}$$

the ideal object to study is:

- **nearby: small Distance D,**
- **massive: large M_{DM} (in FOV),**
- **quiescent: low astrophysical background.**

Astrophysical X-ray Sources:

Stellar Sources:

HMXB:

Fueled by stellar wind; widely-separated

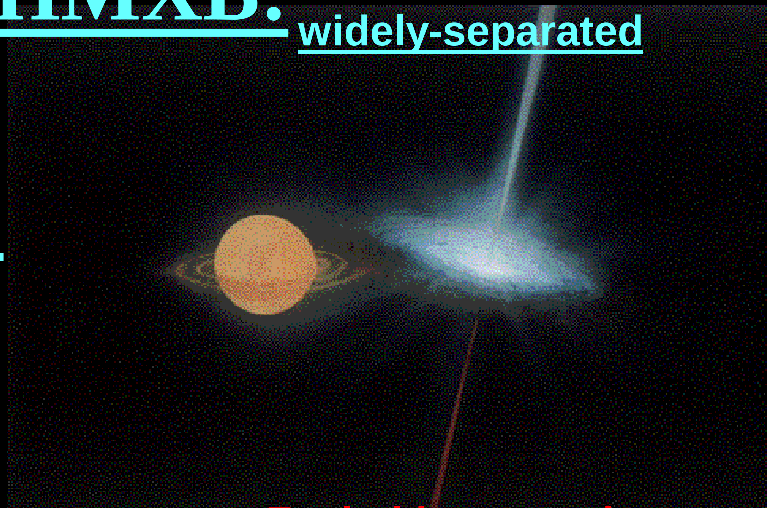

LMXB:

Roche Lobe accretion; Contact Binary systems

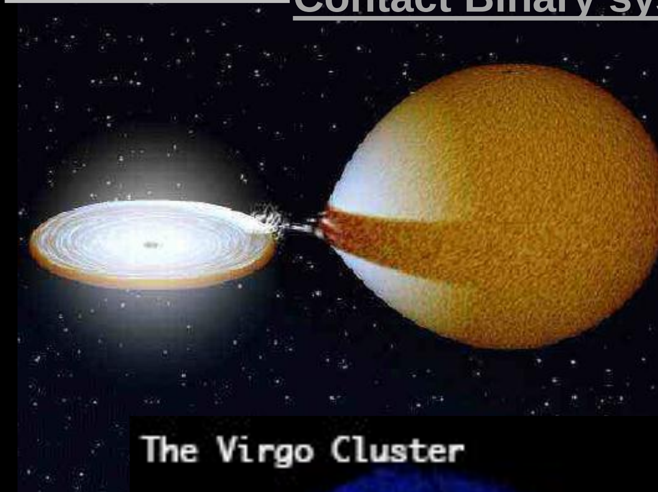

Nuclear & Diffuse Sources:

AGN:

Fueled by accretion onto Supermassive BHs

Hot Gas:

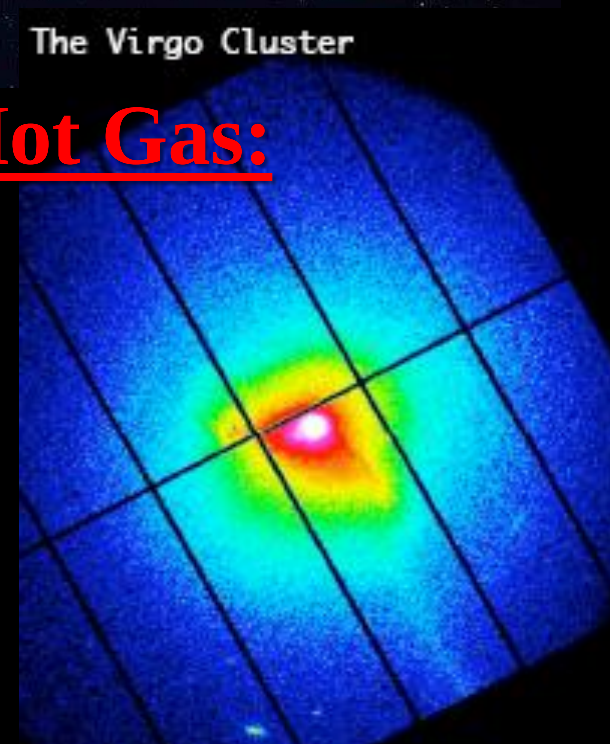

Previous work I: Cosmic X-ray Background

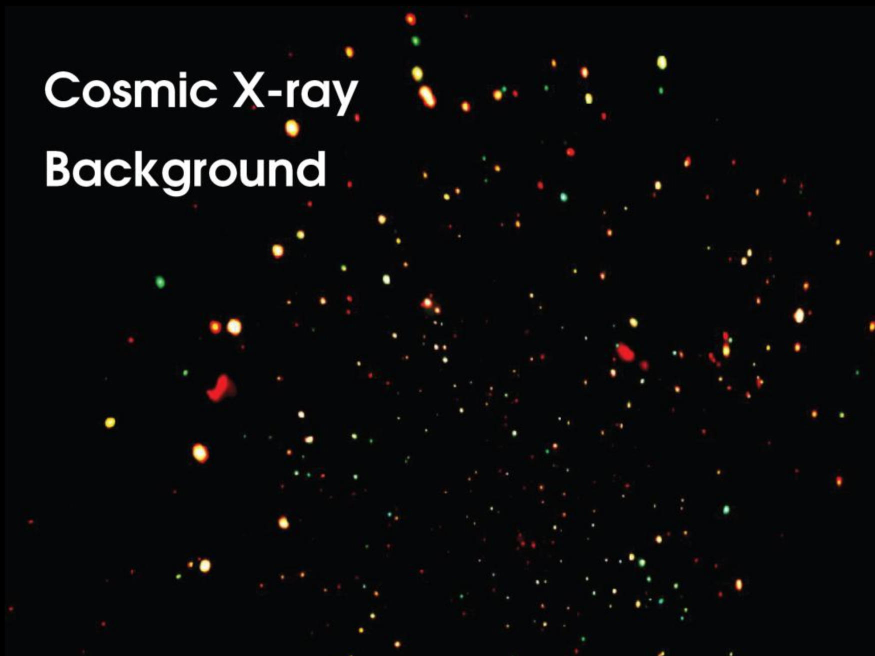

HUGE range of m_s - $\sin^2 2\theta$ probed via combined XMM & HEAO-I Data [61].

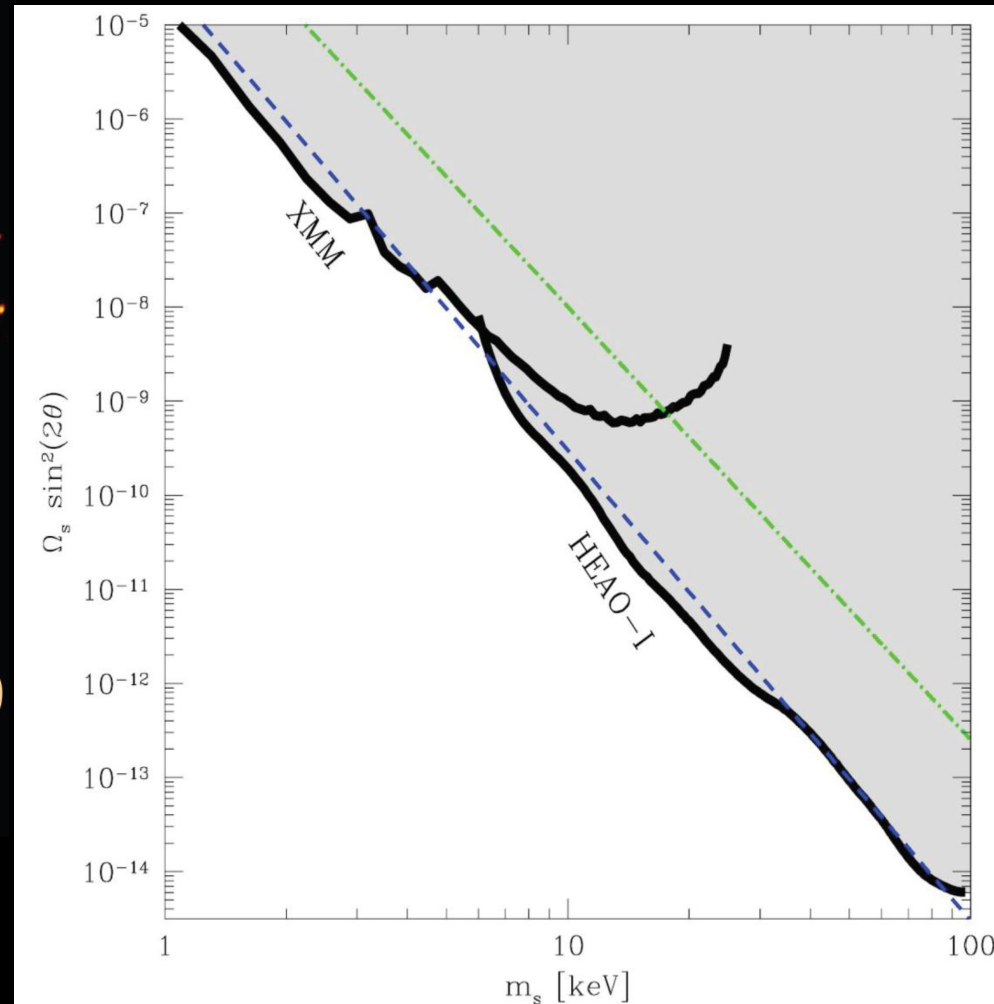

Rekindled interest in m_s X-ray constraints [6].

Constraints: m_s < 9.3 keV

(for DW Model ν_s [3, 43]).

Previous work II: Galaxy Clusters

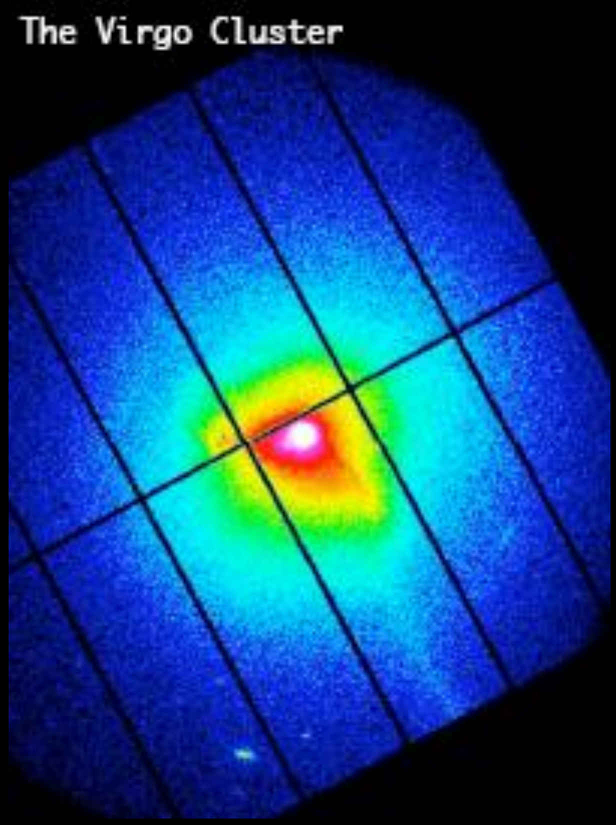

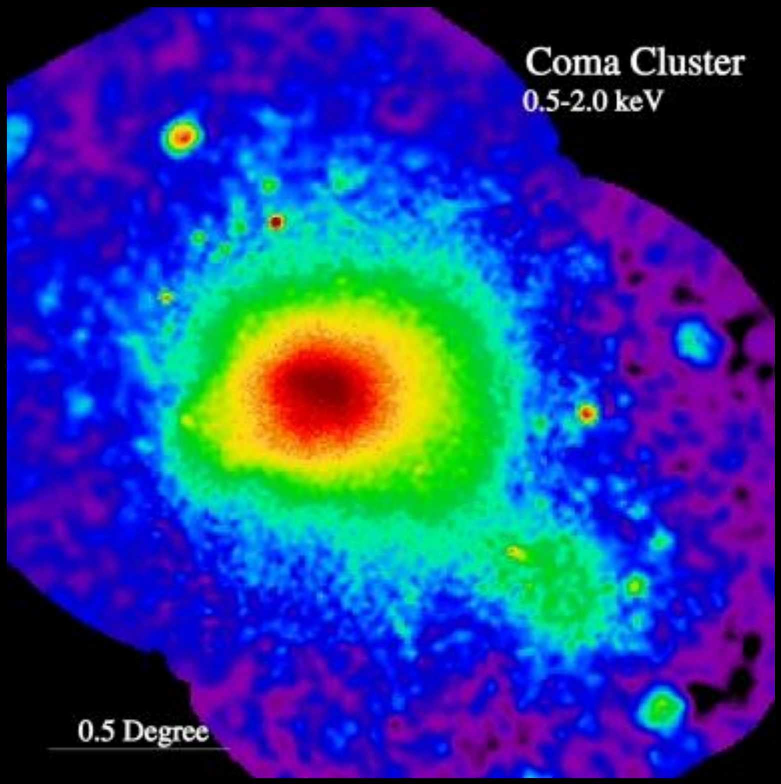

Advantage: HUGE $M_{DM} \sim 10^{13} M_{\odot}$

PROBLEMS: HUGE background; D > 10 Mpc

Constraints (for DW Model ν_s [3, 43]):

m_s < 8.2 keV (Virgo [44]); m_s < 6.3 keV (Virgo + Coma [13, 63]).

Advantages of Andromeda (M31)

(Watson, Li, Polley 2012, Watson, Beacom, Yuksel, Walker 2006 [66])

Nearby: D = 0.78 ± 0.02 Mpc [102, 103]

LOW astrophysical background (little hot gas & bright point sources can be excised)

Well-measured Dark Matter Distribution based on analyses of extensive Rotation Curve Data

(Klypin, Zhao, Somerville 2002 [104], Seigar, Barth, & Bullock 2007 [105])

Prospective Sterile Neutrino Signals

Comparable to Massive Clusters without the background

Exceeding Ultra Nearby Dwarf Galaxies

$$\frac{\Phi_{\mathrm{M31}}}{\Phi_{\mathrm{Clus}}} = \left(\frac{M_{M31}^{FOV}}{M_{\mathrm{Clus}}^{FOV}}\right)\left(\frac{D_{\mathrm{Clus}}}{D_{\mathrm{M31}}}\right)^2 \backsimeq \frac{\Phi_{\mathrm{M31}}}{\Phi_{\mathrm{Dwarf}}} = \left(\frac{M_{M31}^{FOV}}{M_{\mathrm{Dwarf}}^{FOV}}\right)\left(\frac{D_{\mathrm{Dwarf}}}{D_{\mathrm{M31}}}\right)^2 \gtrsim 1$$

Unresolved 5' *XMM* Spectrum of Andromeda

(from Shirey et al. 2001 [96])

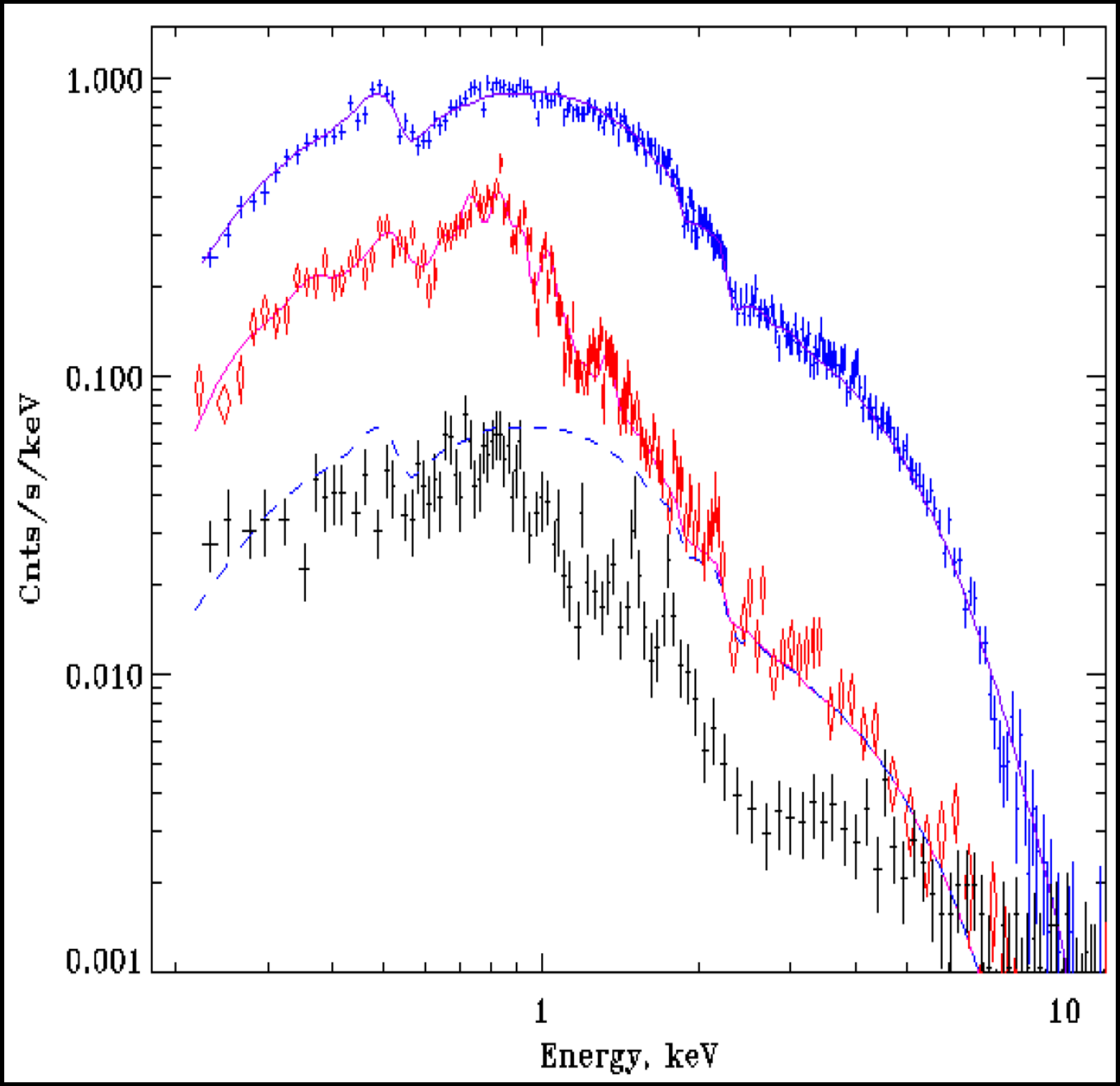

REDUCED Astrophysical Background:

Bright point sources *removed* **(in Ref. [96])**

Intrinsically LOW
hot gas emission

RESULTS

For Ω_s = 0.24 & L = 0 density-production relationship [43]:

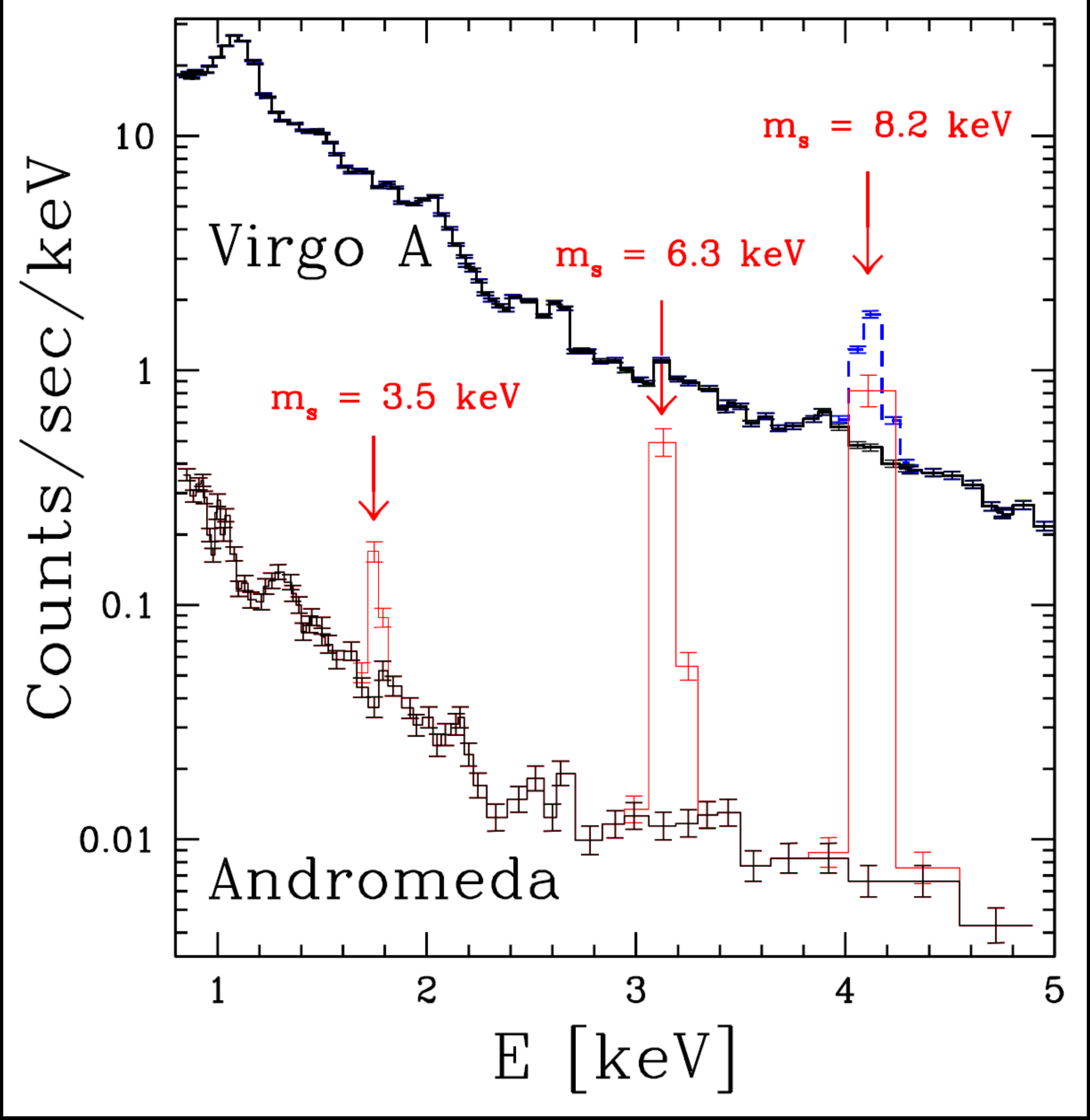

Andromeda:

m_s < 3.5 keV

[66]

Virgo A:

m_s < 8.2 keV

[44]

Virgo A+Coma:

m_s < 6.3 keV

[13, 63]

m_s = 6.3 keV & m_s = 8.2 keV decay peaks are also shown relative to Andromeda data.

Previous work III: Dwarf Galaxies

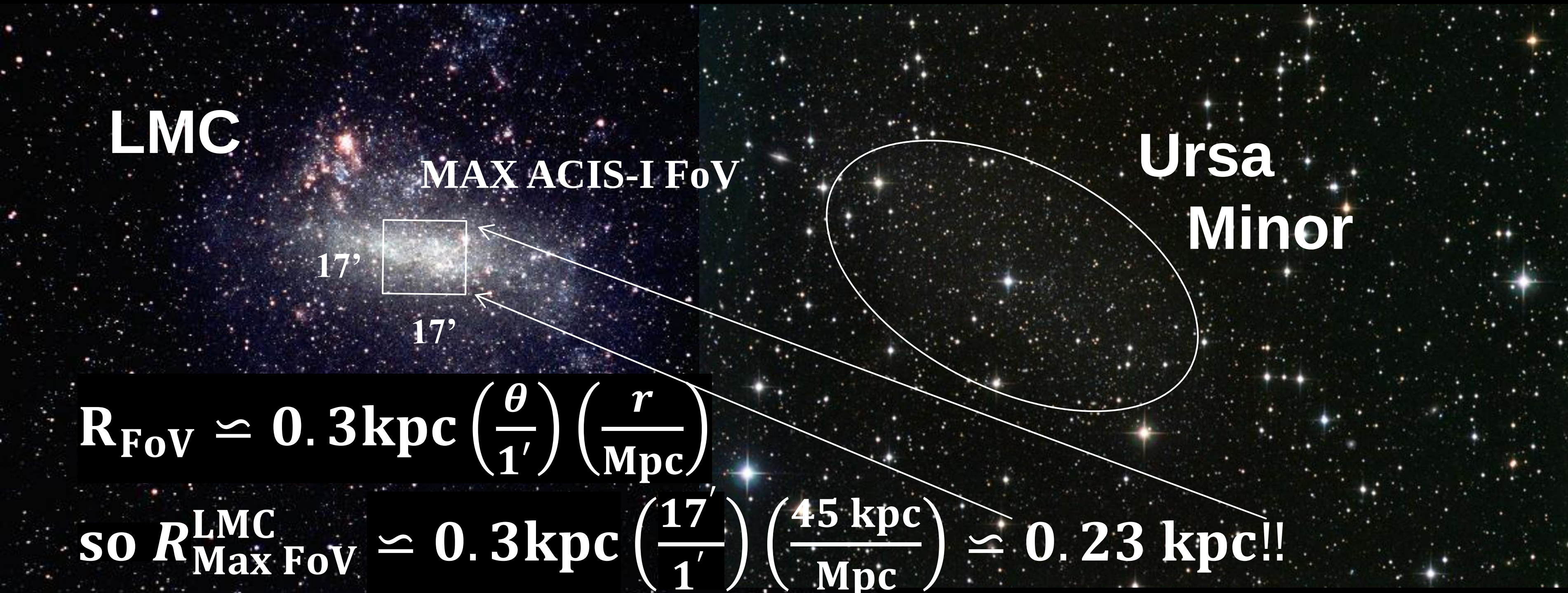

$$\mathrm{R_{FoV}} \backsimeq 0.3\mathrm{kpc}\left(\frac{\theta}{1'}\right)\left(\frac{r}{\mathrm{Mpc}}\right)$$

so $R^{\mathrm{LMC}}_{\mathrm{Max\ FoV}} \backsimeq 0.3\mathrm{kpc}\left(\frac{17'}{1'}\right)\left(\frac{45\ \mathrm{kpc}}{\mathrm{Mpc}}\right) \backsimeq 0.23\ \mathrm{kpc}$!!

Advantages: Small D; Low background

PROBLEMS: Low & Uncertain M_{DM} in FOV.

Constraints (for DW Model ν_s [3, 43]):

m_s < 3 keV** (LMC + MW) [69]

** VERY WEAK EXCLUSION CRITERION

Andromeda (*XMM*) vs. Dwarf/MW Constraints

Andromeda [66] & **LMC + MW** [69]

(Watson, Beacom, Yüksel, Walker 2006)

(Boyarsky, Neronov, Ruchayskiy, Shaposhnikov, Tkachev 2006)

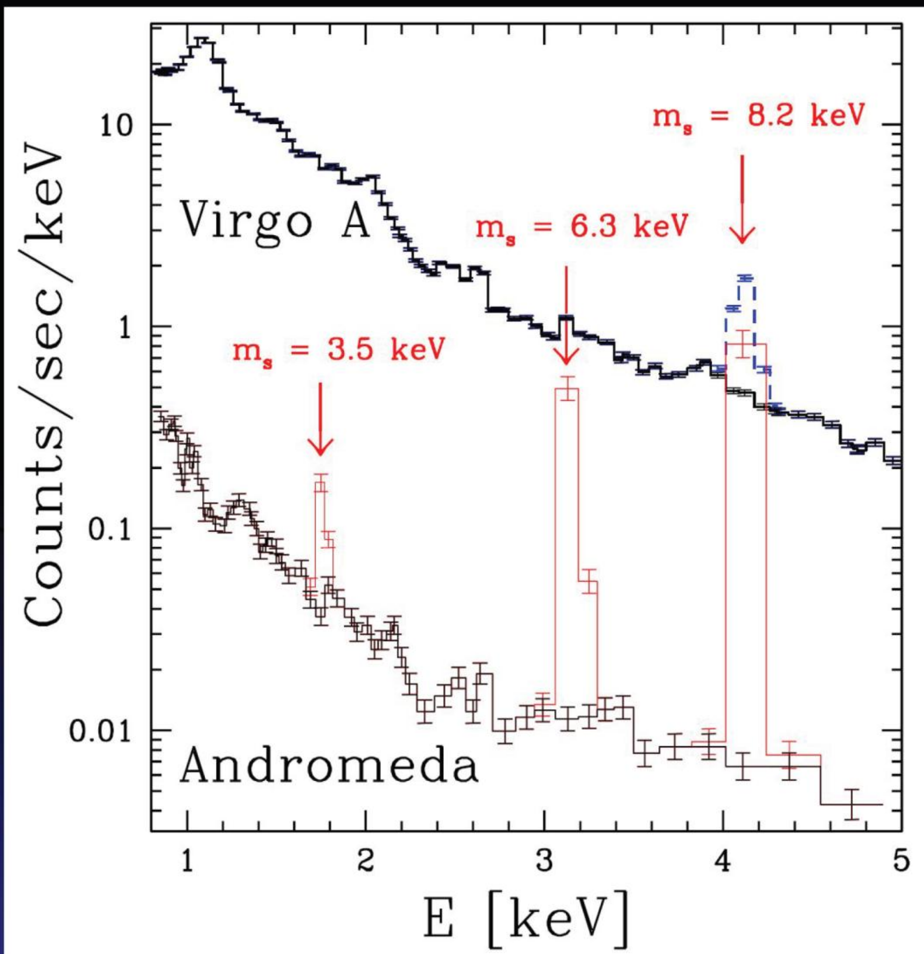

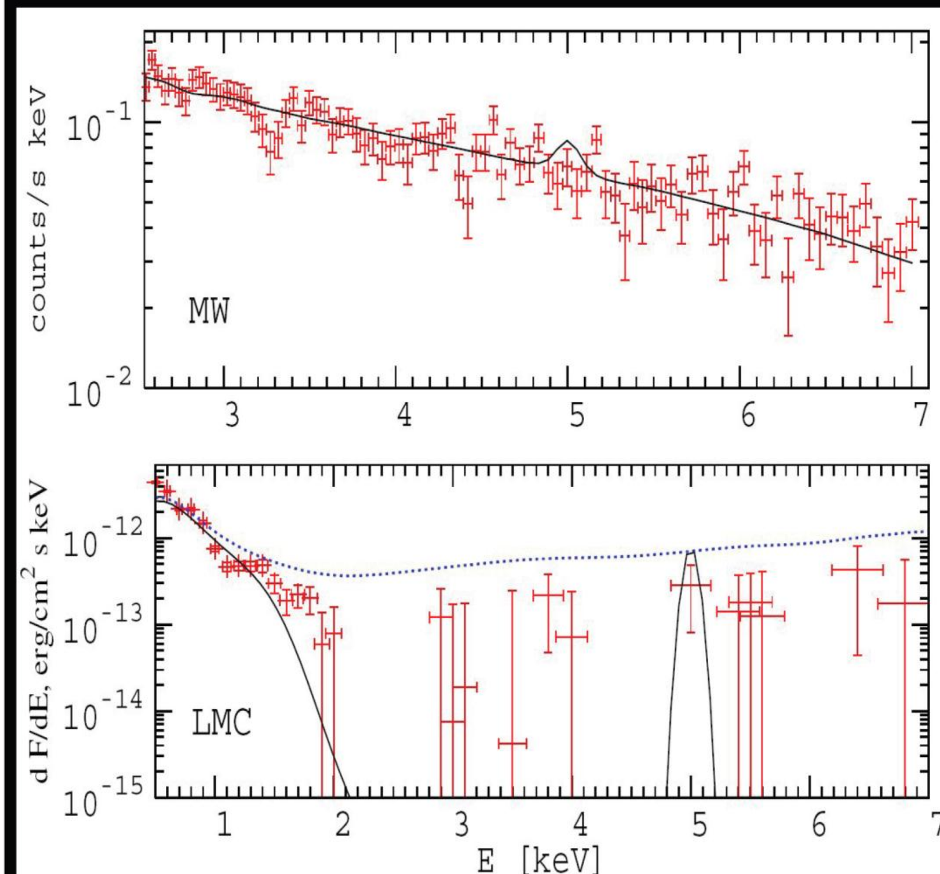

Andromeda (*XMM*) vs. Cluster/Dwarf/MW

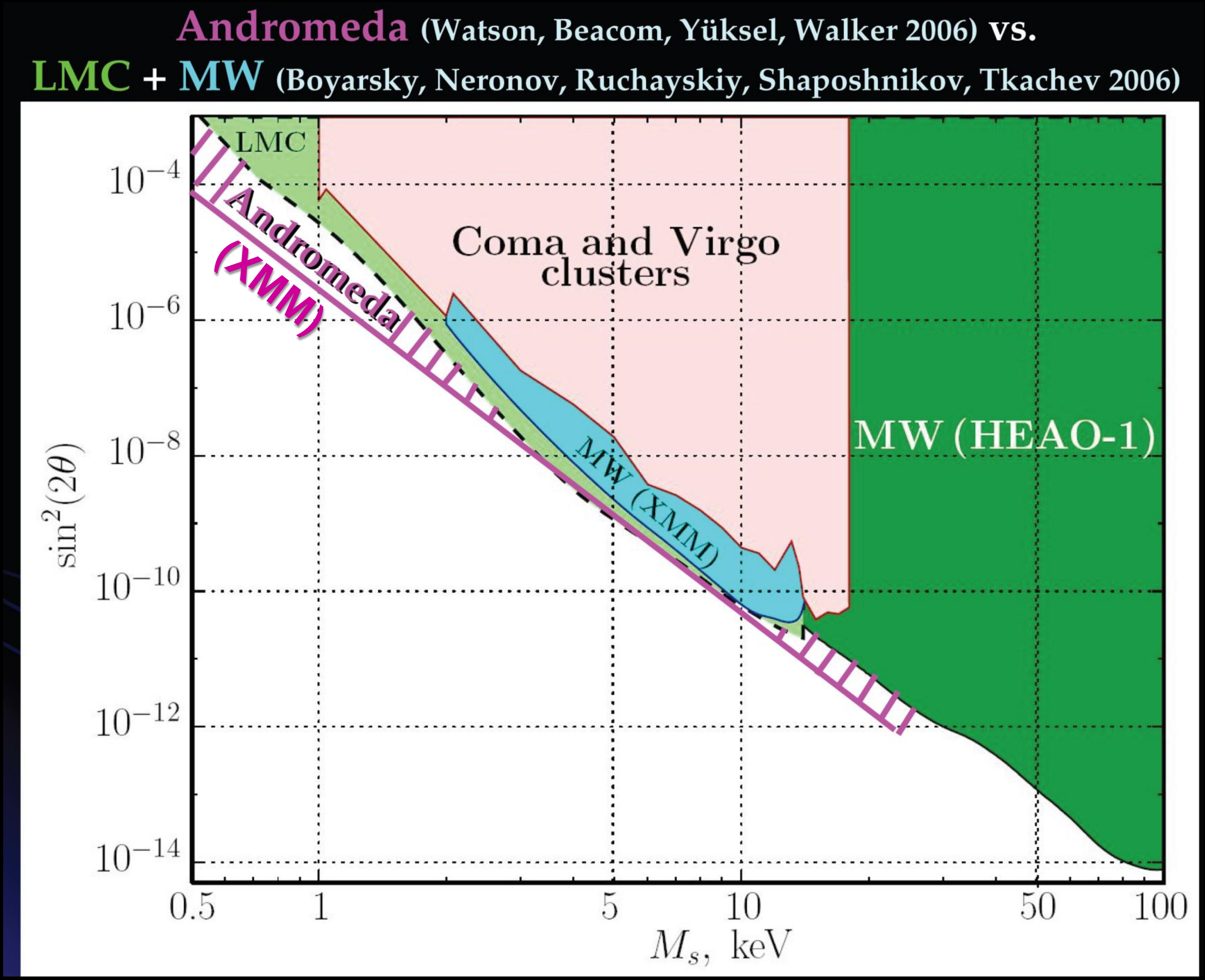

Chandra FOV of M31: $\Delta\theta = 12' - 28'$

- Raw counts associated with the 7 Chandra ACIS-I exposure regions.

- Exposure times range from 5ks to 20ks

- Central 12' is excluded because of high astrophysical background from hot gas and point sources in that region

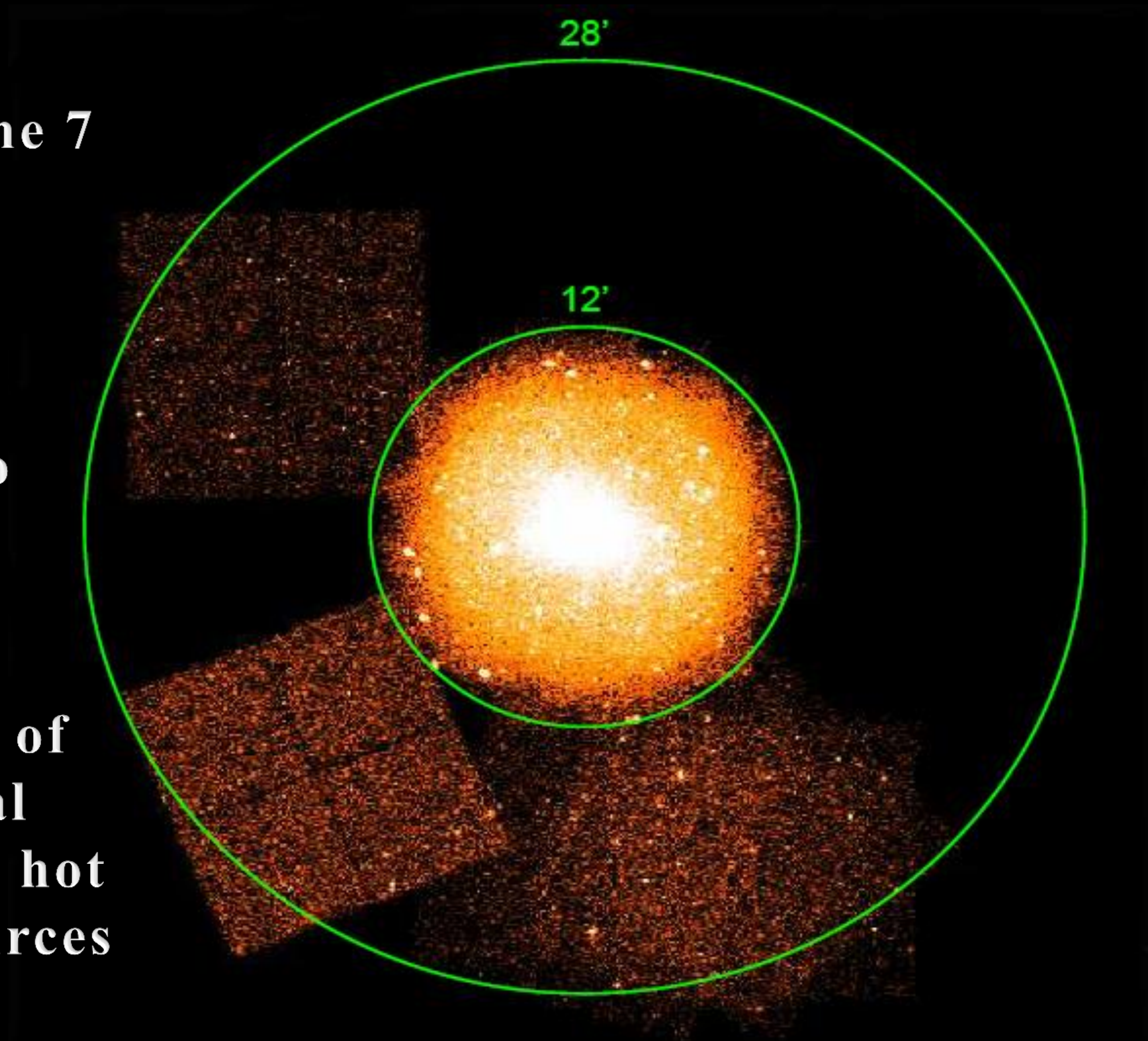

Andromeda's
Well-measured Matter Distribution:

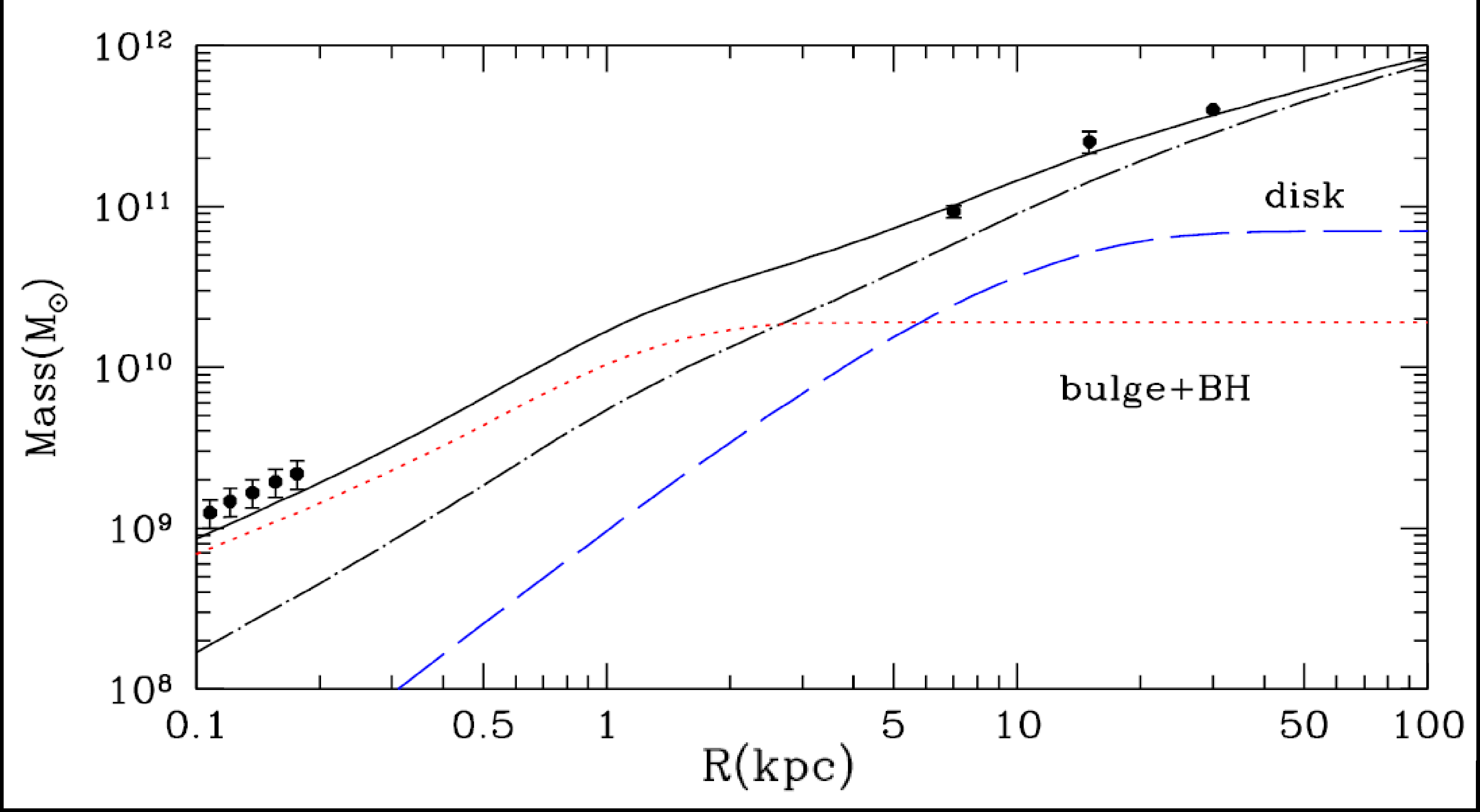

Constraints at small radii are from Stellar Motions in the Nucleus.
Three points at R>5 kpc characterize the spread in v_{rot} = 255 $\pm$ 15 km/s.

(Klypin, Zhao, Somerville 2002 [104] (KZS))

(Additional Data & updated analysis in Seigar, Barth, & Bullock 2007 [105] (SBB))

More Conservative DM Matter Distribution:

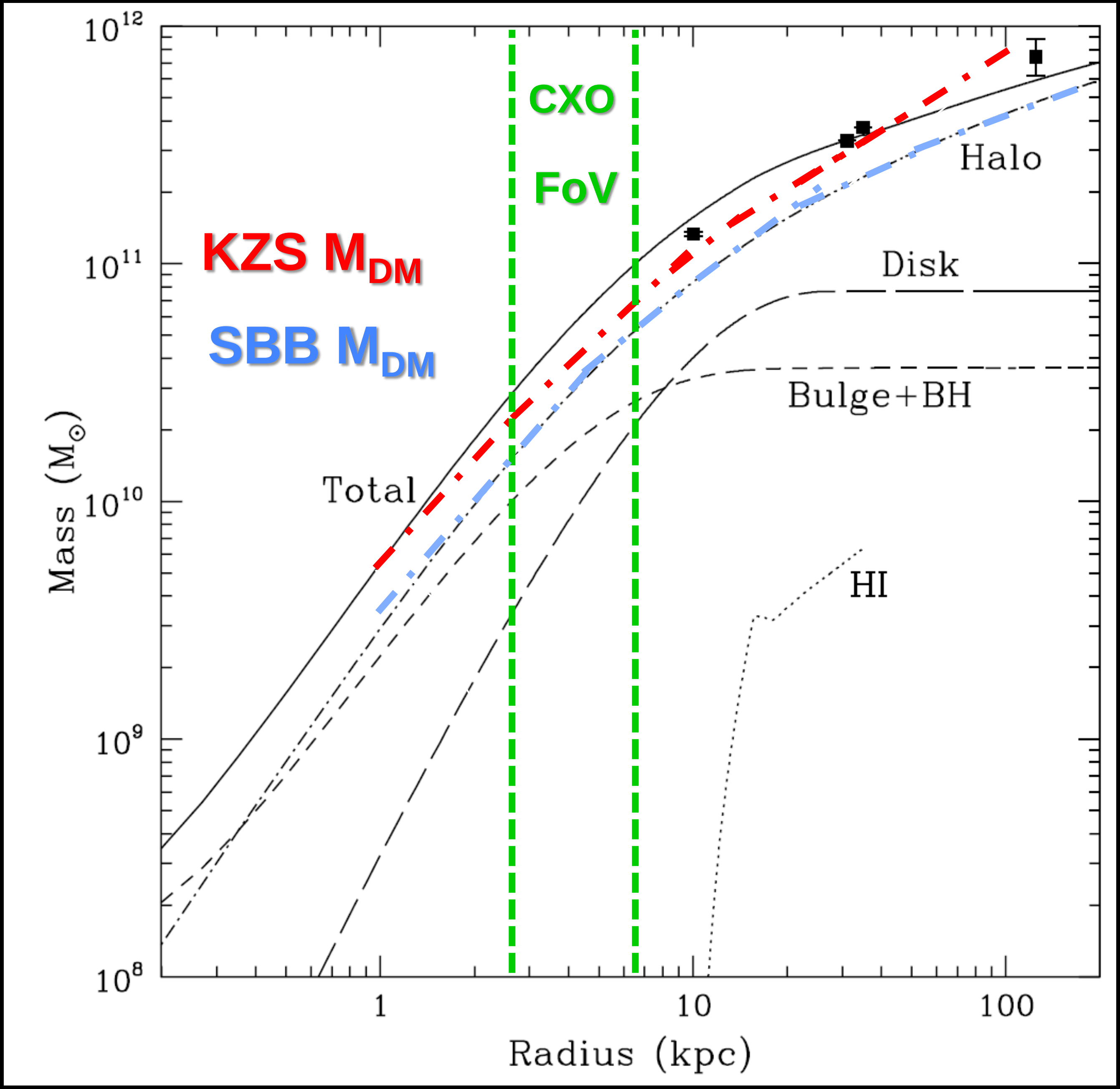

SBB M_{DM} < KZS M_{DM} by a factor of ~ 1.05 – 1.2 in *Chandra* FoV

SBB M_{DM} < Burkert M_{DM} [67, 106] by a factor of ~ 1.2 – 1.4 in *Chandra* FoV

The Fraction of Andromeda's Dark Matter Mass in the *Chandra* field of view (FOV):

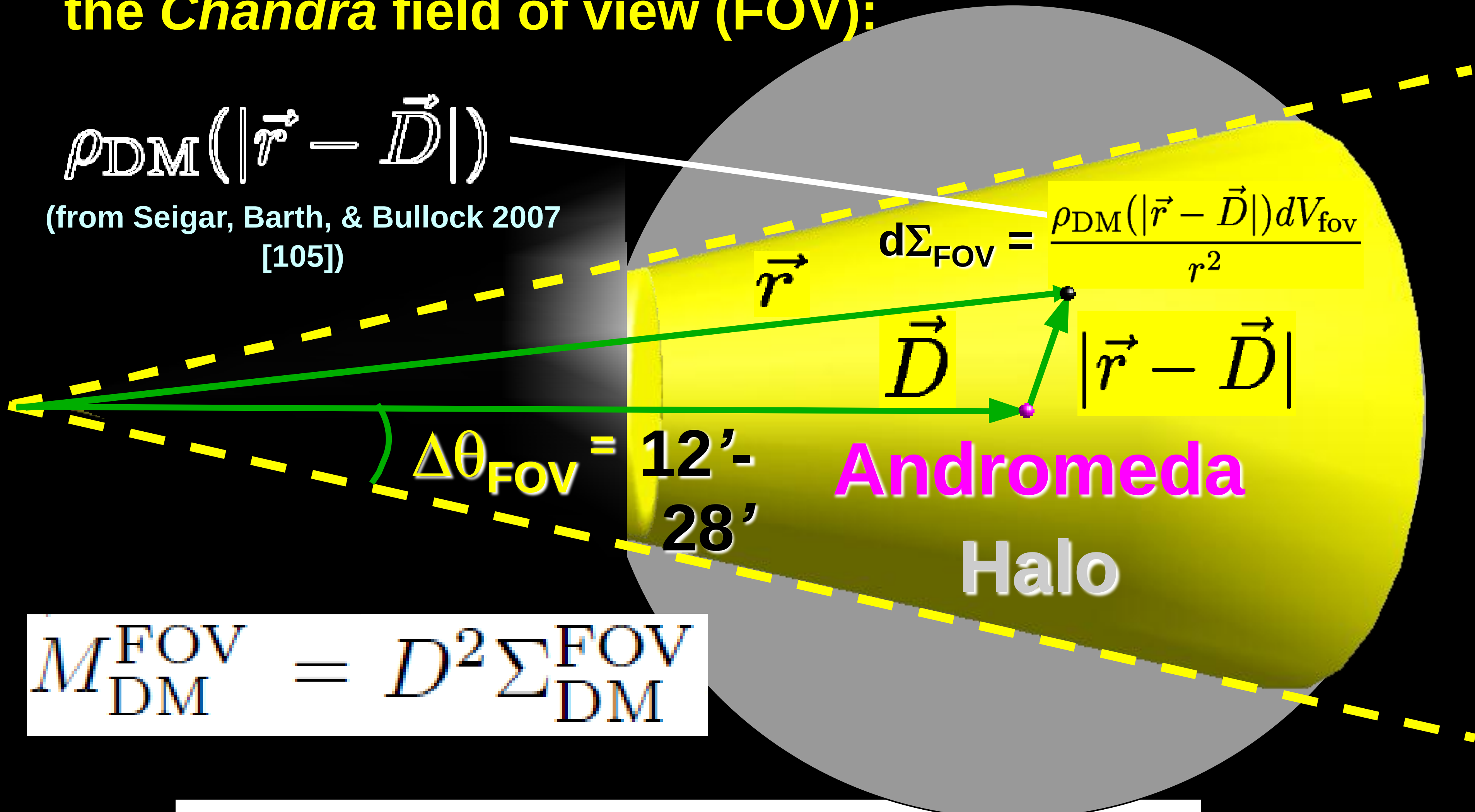

$$M_{\rm DM}^{\rm FOV} = D^2 \Sigma_{\rm DM}^{\rm FOV}$$

$$\Sigma_{\rm DM,M31}^{\rm FOV} \simeq (0.8 \pm 0.04) \times 10^{11} M_{\odot} {\rm Mpc}^{-2}$$

$$M_{\rm DM,M31}^{\rm FOV} \simeq (0.49 \pm 0.05) \times 10^{11} M_{\odot}$$

Conversion of Decay Signal to Detector Units:

$$\frac{dN_{\gamma,\mathrm{s}}}{dE_{\gamma,\mathrm{s}}dt}(\Omega_\mathrm{s}) = \left(\frac{\Phi_{\mathrm{x,s}}(\Omega_\mathrm{s})}{E_{\gamma,\mathrm{s}}}\right)\left(\frac{A_\mathrm{eff}(E_{\gamma,\mathrm{s}})}{\Delta E}\right)$$

$$= 6.7\times 10^{-2}\ \mathrm{Counts/sec/keV}\left(\frac{\mathrm{A_{eff}(E_{\gamma,s})}}{100\ \mathrm{cm}^2}\right)$$

$$\times\left(\frac{\Sigma^{\mathrm{FOV}}_{\mathrm{DM}}}{10^{11}M_\odot\mathrm{Mpc}^{-2}}\right)\left(\frac{\Omega_\mathrm{s}}{0.24}\right)^{0.813}\left(\frac{m_s}{\mathrm{keV}}\right)^{1.374}$$

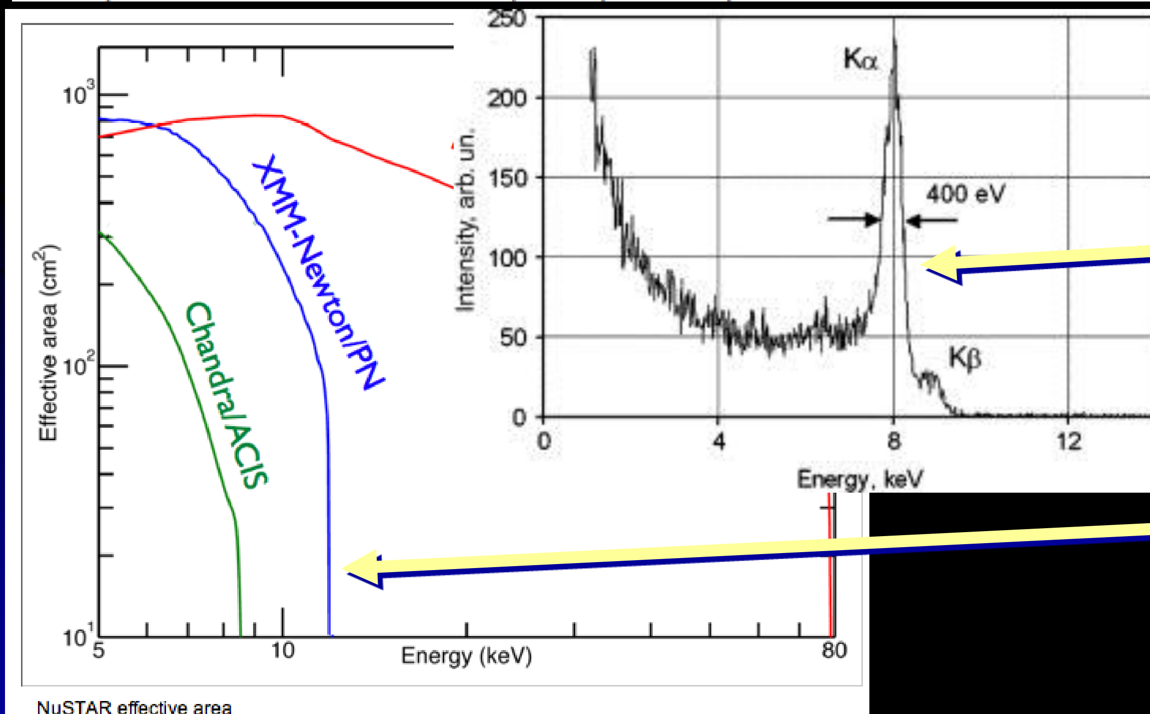

Detection of ν_s Decays at $E_{\gamma,s}$ depends on

- $\Phi_{x,s}$
- Spectral Energy Resolution $\Delta E \simeq E/15$
- ACIS-I Effective Area $A_{eff}(E_{\gamma,s})$

Detection/Exclusion Criterion:

$$\frac{dN_{\gamma,\mathrm{s}}}{dE_{\gamma,\mathrm{s}}dt}(\Omega_{\mathrm{s}}) \geq \Delta\mathcal{F}$$

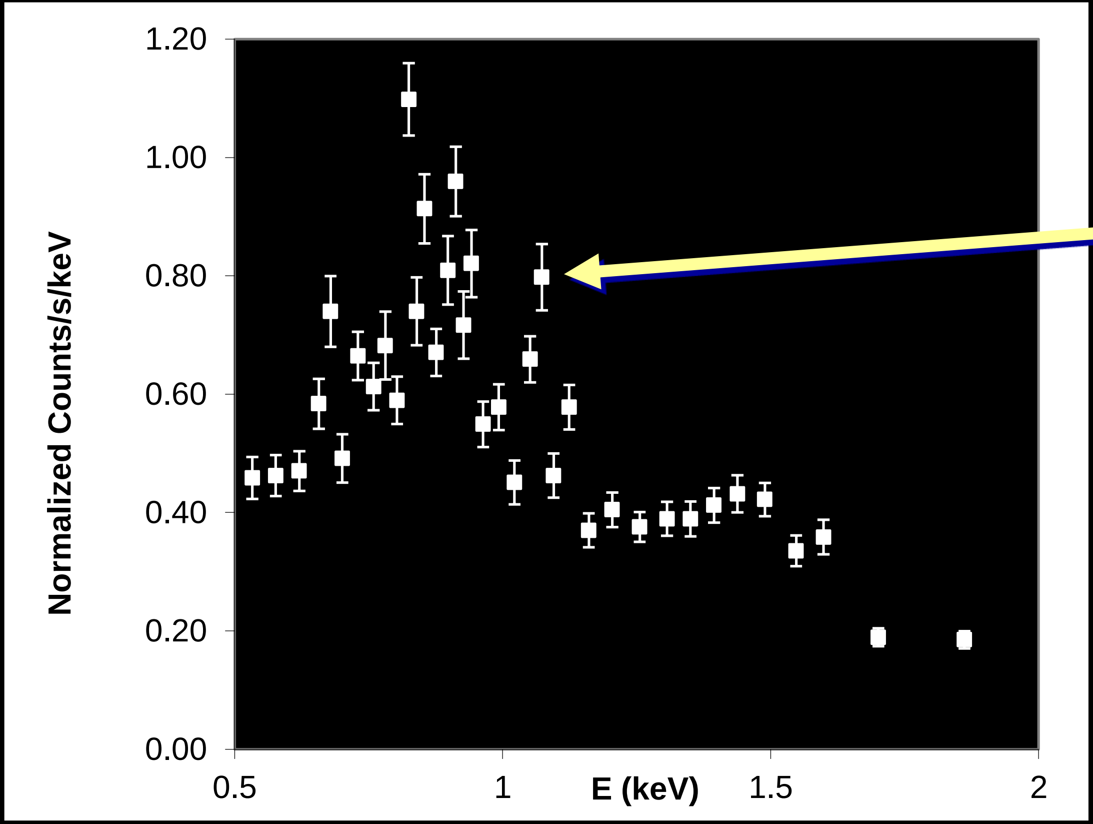

- **Sterile Neutrino Decay Signal** $dN_{\gamma,s}/dE_{\gamma,s}dt$
- **$\geq$ *Chandra* Data** $\Delta\mathcal{F}$
- **in a given bin of energy** $E_{\gamma,s}$

Limits on m_s from *Chandra* Observations of M31

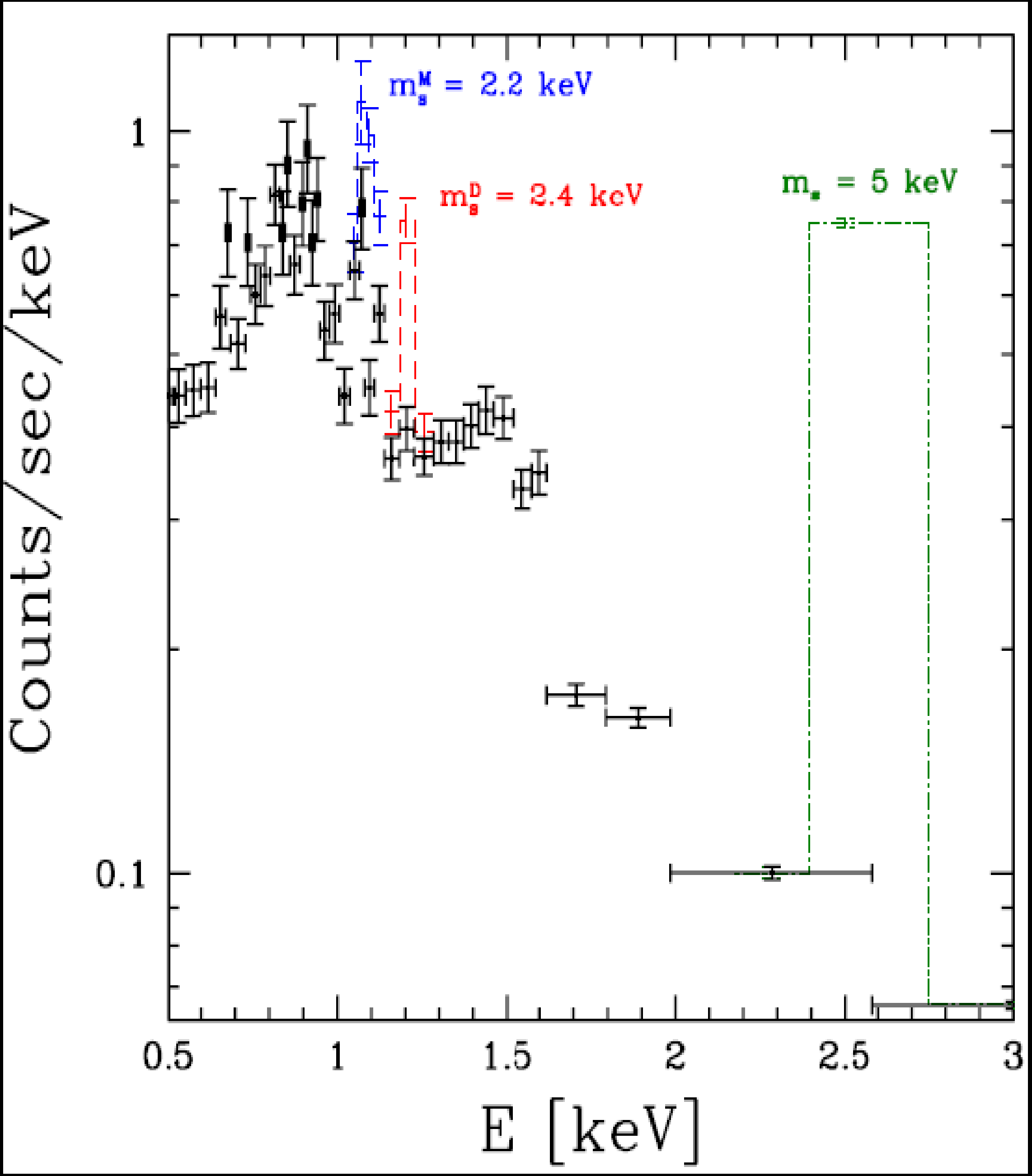

Chandra **unresolved X-ray spectrum emitted from 12' - 28' annular region of Andromeda (M31).**

Majorana:

m_s < 2.2 keV

Dirac:

m_s < 2.4 keV

Claimed Detection:

m_s = 5 keV

(Loewenstein & Kusenko 2010 [82]) STRONGLY excluded by our data!

Generalized constraints in the m_s – $\sin^2 2\theta$ plane

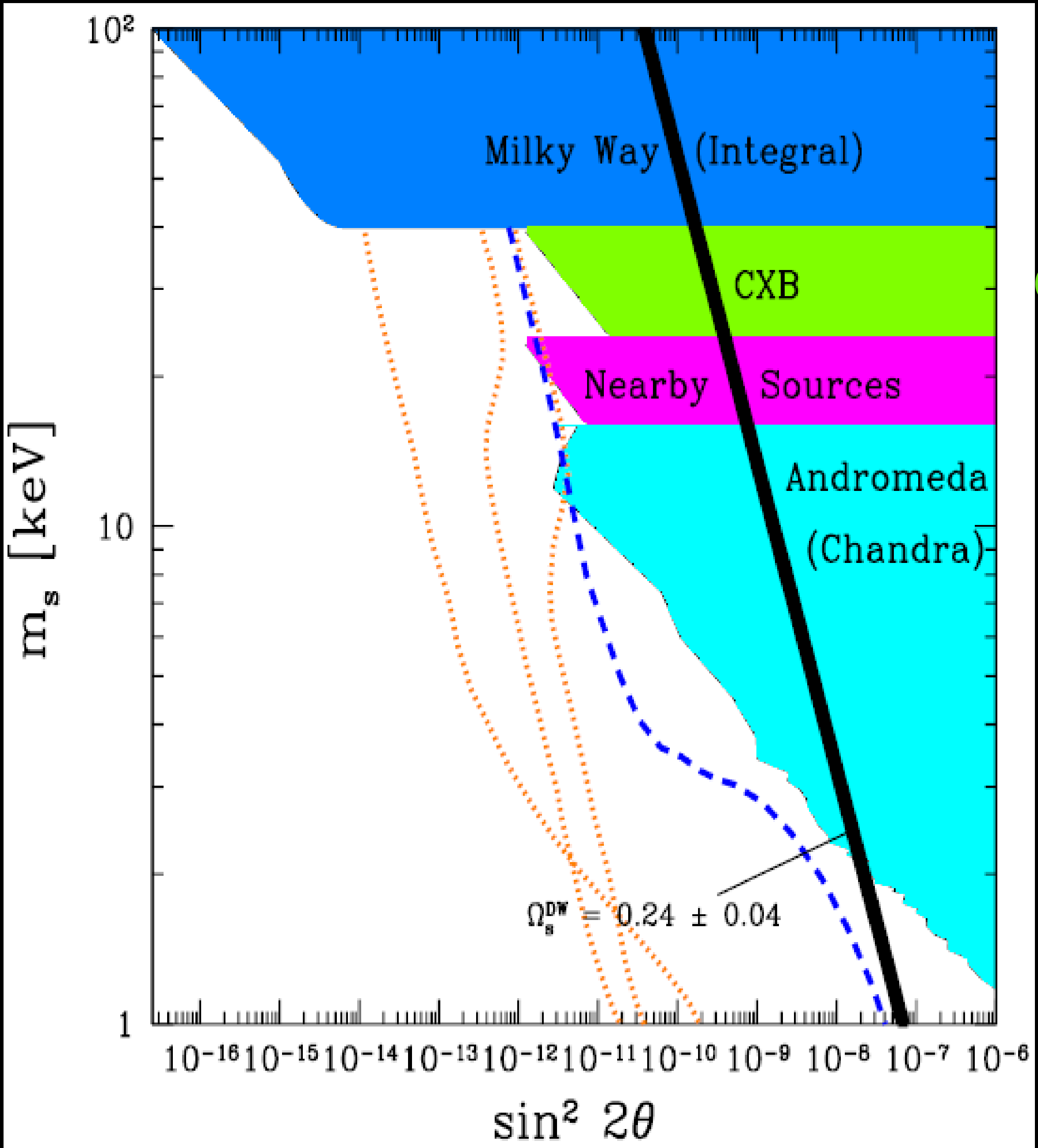

Exclusion Regions:

Milky Way (Integral):

[77, 78]

Cosmic X-ray Background:

[61,62]

Andromeda (XMM):

[66]

Andromeda (CXO):

(Watson, Li, & Polley 2012)

Density-Production Models:

Dodelson-Widrow Model

[3]

Shi-Fuller Model

[4, 53]

3 L >> 10^{-10} Lines

[13]

Summary I

Our *Chandra* M31 Constraint (at L=0): m_s < 2.2 keV

+

Tremaine-Gunn Bound: m_s > 0.4 keV

(Tremaine & Gunn 1979 [108])

restricts m_s to a narrow window

consistent with the range of m_s values

that best explains the core of the

Fornax Dwarf Spheroidal Galaxy.

(Strigari, et al. 2006 [109])

Higher mass ν_sWDM also remains viable if

the Lepton Asymmetry is very large, i.e., L >>10^{-10}

(Abazajian & Koushiappas 2006 [13])

Issues with Current Detectors I

Need **larger effective Area** to offset diminishing decay signal

$$\frac{dN_s}{dE_\gamma dt} \propto E_\gamma^{1.374}$$

against rising backgrounds at lower Eγ.

And **improved ΔE** to distinguish adjacent lines.

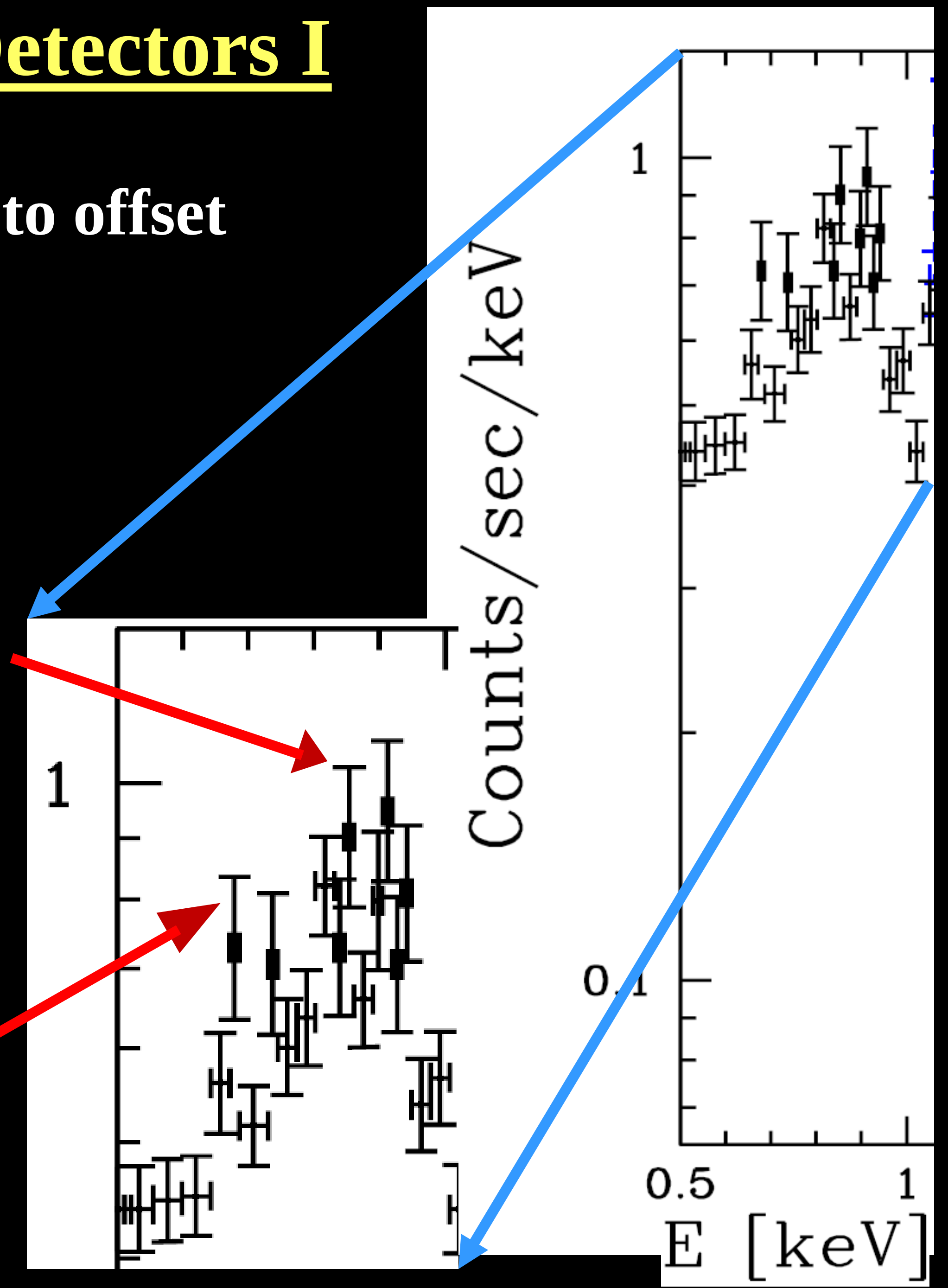

Prospects for Future Constraints:

IXO Observations of Andromeda (Abazajian 2009 [111])

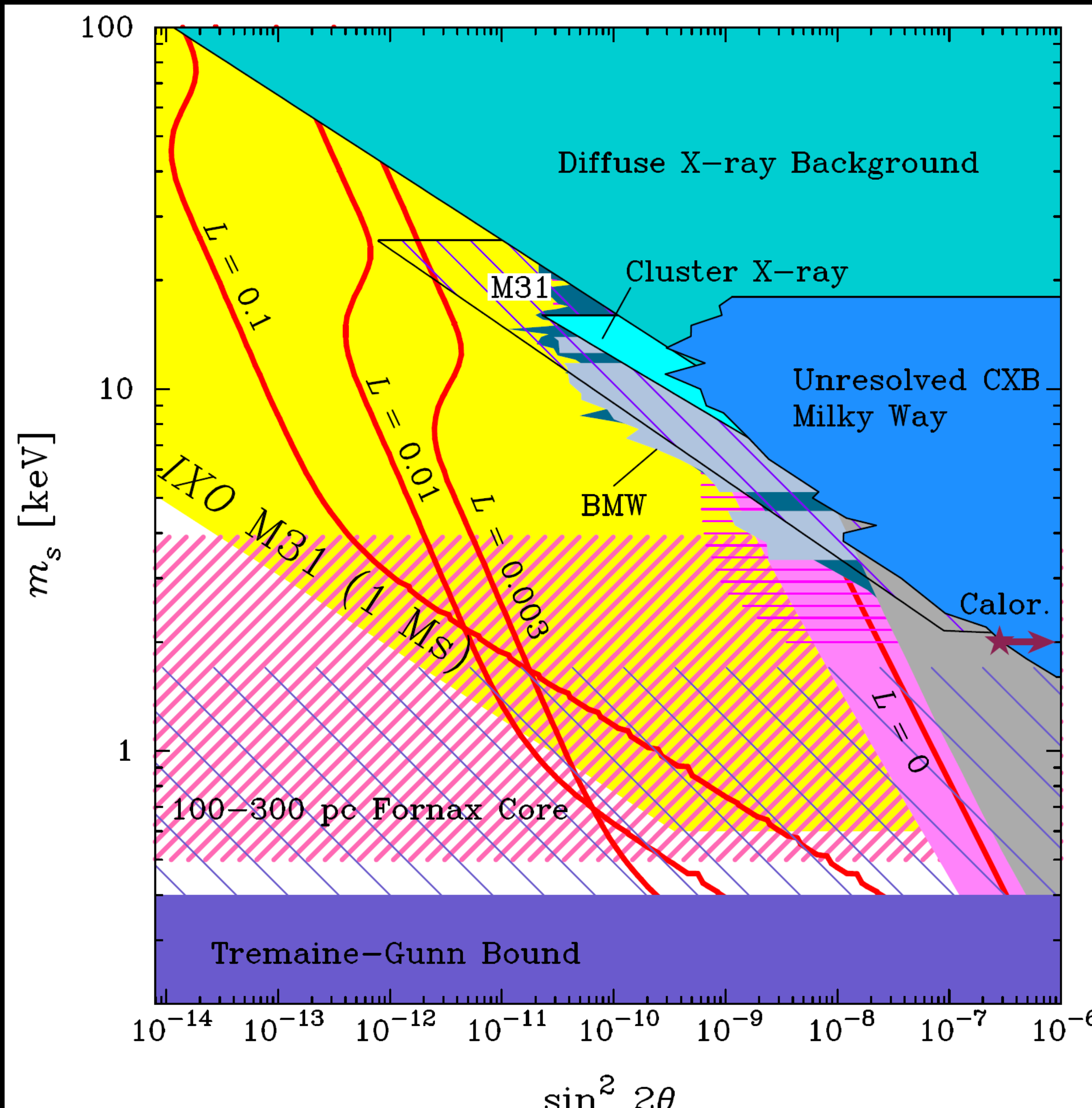

IXO vs. *Chandra*

- ~ comparable FOV
- ~ 100 X larger A_{eff}
- ~ 10 X better ΔE
- ~ 10 X lower instrumental background
- ~1 Ms observation of M31 can *significantly* improve sterile neutrino constraints.

* Similar for ATHENA*

Summary II

Current *Chandra* Constraints: $m_s < 2.2$ keV are close to the limit of contemporary detectors.

Long-term progress will require next-generation instruments with greatly improved A_{eff} & ΔE.

To make near-term progress, examine nearby systems with the potential for large amounts of spatially separated dark matter – such as prospective DM filaments in merging galaxies, i.e., M81/M82.

Cons – DM masses not testable by lensing; minimal improvements

Phase Space Density Basics

$$Q = \frac{\rho}{\sigma^3}$$

- For a fermionic thermal relic, Hogan & Dalcanton [1] find:

$$Q_{Thermal} = 5 \times 10^{-4} \frac{(M_{\odot}/pc^3)}{(km\, s^{-1})^3} (M_X/1keV)^4$$

- adiabatic invariant
- strongly mass-dependent

Connecting the Past to the Present

- Galaxy formation processes alter Q by an unknown factor Z:

$$Z = \frac{Q_{primordial}}{Q_{today}} = \frac{Q_P}{Q_0}$$

- De Vega & Sanchez [2] explored a number of analytical methods to find Z, concluding that
  - $1 \leq Z \leq 10^4$, in agreement with simulations
  - the mass of a thermal relic DM particle is ~ keV:

$$m \propto (ZQ_0)^{1/4} \simeq 1-10\,\text{keV}.$$

Goals of Our Project

1. Determine Z directly from the dwarf galaxy data to produce a model-independent mapping between Q_p and Q_0

2. Use this Z factor to reduce the uncertainty on the dark matter particle mass from a factor of 10 to a factor of ~ 2.

Dwarf Galaxy Data

- Lowest uncertainty data from Walker et. al. [3]

Dwarf	σ (km/s)			ρ (M_Θ pc^{-3})			r_{hf} (pc)			$M(r_{hf})$ (10^7 M_Θ)		
Carina	6.6	±	1.2	0.1	±	0.04	241	±	23	0.61	±	0.23
Draco	9.1	±	1.2	0.3	±	0.08	196	±	12	0.94	±	0.25
Fornax	11.7	±	0.9	0.042	±	0.007	668	±	34	5.3	±	0.9
Leo I	9.2	±	1.4	0.19	±	0.06	246	±	19	1.2	±	0.4
Leo II	6.6	±	0.7	0.26	±	0.06	151	±	17	0.38	±	0.09
Sculptor	9.2	±	1.1	0.17	±	0.05	260	±	39	1.3	±	0.4
Sextans	7.9	±	1.3	0.019	±	0.007	682	±	117	2.5	±	0.9
U Minor	9.5	±	1.2	0.16	±	0.04	280	±	15	1.5	±	0.4
C Ven I	7.6	±	0.4	0.025	±	0.003	564	±	36	1.9	±	0.2
U Ma II	6.7	±	1.4	0.32	±	0.14	140	±	25	0.36	±	0.16

Q – r_{hf} Power-Law Relation

- The power-law relations from Walker et al. [3]:

$$\rho \propto r_{hf}^{-1.6}; \sigma \propto r_{hf}^{0.2} \rightarrow \quad Q = \frac{\rho}{\sigma^3} \propto r_{hf}^{-2.2}.$$

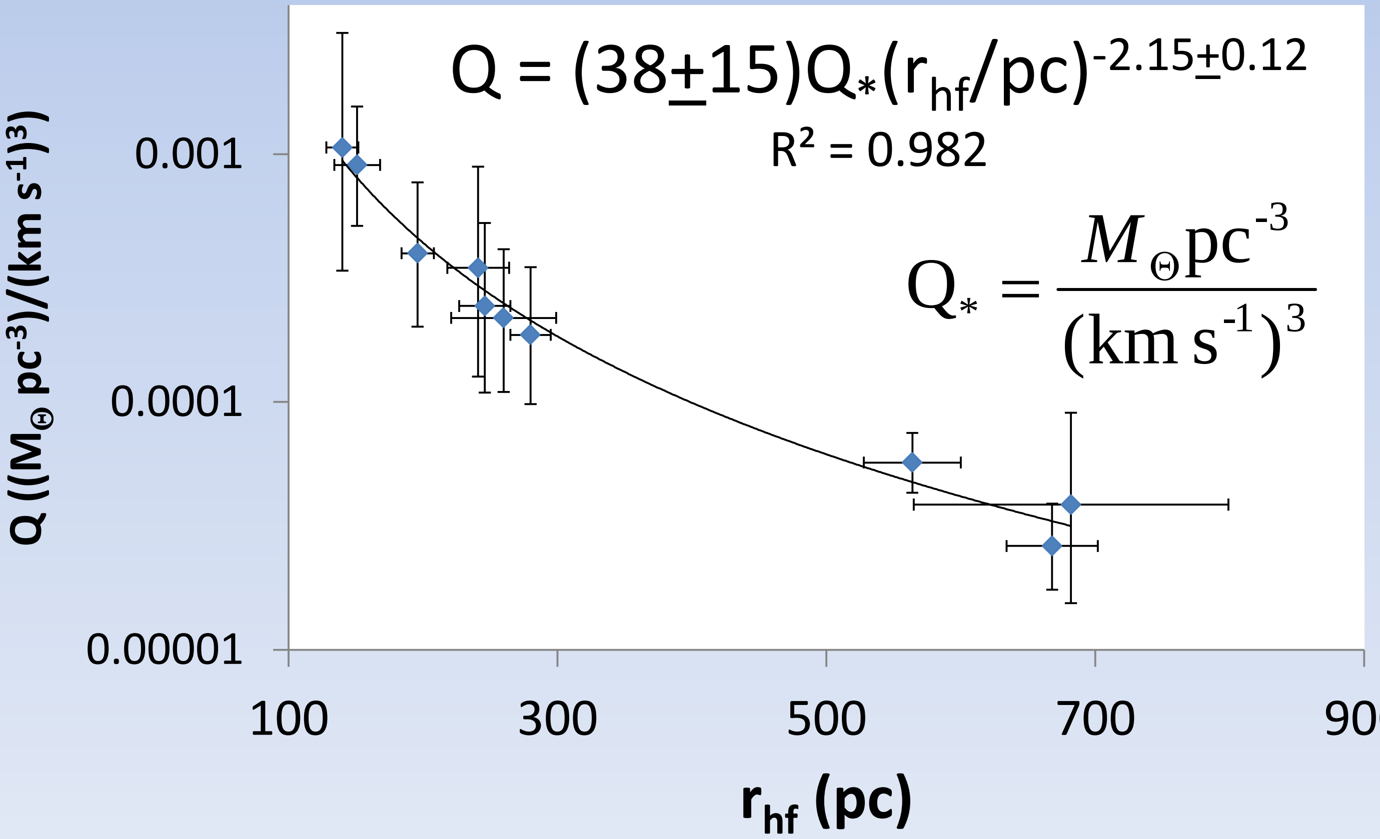

Using $Q(r_{hf})$ to find Z

- We can rewrite the $Q(r_{hf})$ power-law in terms of:
  - the unknown, primordial Q_p

  and
  - an unknown radial scale, r_p:

$$Q_0 = \left(\frac{Q_p}{Z}\right) = Q_p \left(\frac{r_p}{r_{hf}}\right)^n, \text{so } Z = \left(\frac{r_{hf}}{r_p}\right)^n.$$

- Thus, determining r_p is the key to the empirical Z factor.

Finding r_p analytically

- Determine when the virial mass of the MW halo entered the horizon:
  - Earliest time causal processes could affect the PSD of DM in a MW-sized overdensity and in its primordial subhalo overdensities

$$M_{horizon}(z) = \frac{4}{3}\pi\rho_{m,0}(1+z)^3\left(\frac{d_H(z)}{2}\right)^3 = 1.5 \pm 0.5 \times 10^{12} M_\Theta$$

- This occurs when
  - $z = (9.2 \pm 1.0) \times 10^4$
  - $r_p = d_H(z)/2 = 26.5 \pm 6$ pc (90% CL)

Finding r_p empirically

- Exploit the fact that there are two distinct dwarf galaxy subpopulations
  - Group A: low $\sigma = 7.1 \pm 1.1$ km/s
  - Group B: high $\sigma = 9.7 \pm 1.2$ km/s.

Dwarf	σ	(km/s)
Carina	**6.6**	**± 1.2**
Leo II	**6.6**	**± 0.7**
Sextans	**7.9**	**± 1.3**
C Ven I	**7.6**	**± 0.4**
U Ma II	**6.7**	**± 1.4**

$\sigma = 7.1 \pm 1.1$ km/s

Dwarf	σ	(km/s)
Draco	**9.1**	**± 1.2**
Fornax	**11.7**	**± 0.9**
Leo I	**9.2**	**± 1.4**
Sculptor	**9.2**	**± 1.1**
U Minor	**9.5**	**± 1.2**

$\sigma = 9.7 \pm 1.2$ km/s

Low & High σ Populations: A & B

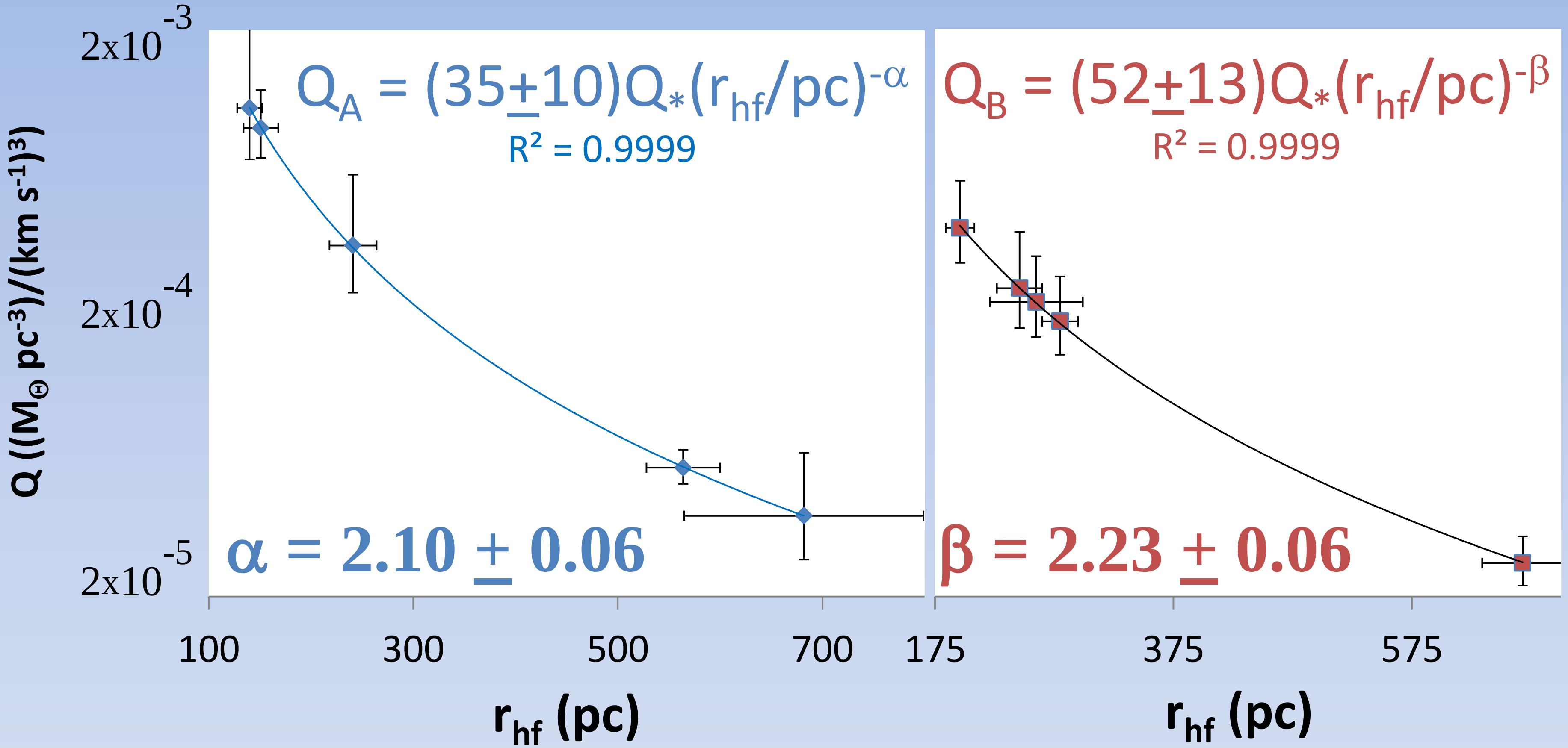

$$Q_A = Q_p\left(\frac{r_p}{r_{hf_A}}\right)^{\alpha} + \; Q_B = Q_p\left(\frac{r_p}{r_{hf_B}}\right)^{\beta} \;\rightarrow\; r_p = r_{hf_A}\left(\frac{Q_B}{Q_A}\left(\frac{r_{hf_B}}{r_{hf_A}}\right)^{\beta}\right)^{\frac{1}{\beta-\alpha}}$$

Empirical r_p Results

- Although $(\beta-\alpha)^{-1}\approx 8$, we find a small range of r_p values:

$$r_p = r_{hf_A}\left(\frac{Q_B}{Q_A}\left(\frac{r_{hf_B}}{r_{hf_A}}\right)^{\beta}\right)^{\frac{1}{\beta-\alpha}} \quad \rightarrow \quad r_p = 24.6 \pm 6 \ \text{pc} \,(95\%\,\text{CL})$$

$$\text{vs.} \ \ r_p = 26.5 \pm 6 \ \text{pc} \,(90\%\,\text{CL})$$

(analytical)

- Consistent Analytical & Empirical r_p values
- Now determine DM mass (for thermal relics):

$$\frac{m}{\text{keV}} = \left(\frac{Q_p}{A}\right)^{1/4} = \left(\frac{ZQ_0}{A}\right)^{1/4} = \left(\left(\frac{r_{hf}}{r_p}\right)^{\gamma}\frac{Q_0}{A}\right)^{1/4}$$

Q_p Values + DM Particle Mass

- Max/Min Q_0 ratio is ~ 41
- Max/Min Q_p differ by < 4%
- Max/Min m differ by < 1%

Including all galaxy data uncertainties

- 30 < Z < 3000
- 2.2 < m/keV < 4.2

Dwarf	Mean Q_0	Mean Q_p	Mean Z	m (keV)
Carina	3.48E-04	0.042	120	3.024
Draco	3.98E-04	0.040	101	2.996
Fornax	2.62E-05	0.041	1555	3.005
Leo I	2.44E-04	0.041	168	3.009
Leo II	9.04E-04	0.041	45	3.003
Sculptor	2.18E-04	0.041	190	3.018
Sextans	3.85E-05	0.041	1069	3.013
U Minor	1.87E-04	0.042	224	3.024
C Ven I	5.70E-05	0.041	717	3.006
U Ma II	1.06E-03	0.041	38	3.006
MAX/MIN	40.6	1.038	40.6	1.009

Results

- Mean thermal relic DM particle mass: 3.0 keV.
- Range of 2.2 - 4.2 keV with all dwarf galaxy measurement uncertainties accounted for (i.e., full range of r_p = 18.5 - 30.5 pc).
- Appealing to the Quasar Luminosity Function, Song and Lee [4] found $0.3 < m/\mathrm{keV} < 3.0$.
- Combining the results: $2.2 < m/\mathrm{keV} < 3.0$

Non-thermal DM

- If the DM particle is a sterile neutrino, we can use the following transformation equations [5] to find the corresponding non-thermal limits:

$$m_\nu^{\mathrm{DW}} = 4.4\mathrm{keV}\left(\frac{m_{\mathrm{Thermal}}}{\mathrm{keV}}\right)^{4/3} \cong 1.5 m_\nu^{\mathrm{SF}} \cong 4.5 m_\nu^{\nu\mathrm{MSM}}$$

- Applying these transformations, we find:

12.6 < m/keV < **19.1** for a DW Sterile Neutrino. **X** **[6]**

8.4 < m/keV < **12.7** for a Shi-Fuller Sterile Neutrino.

2.8 < m/keV < **4.2** for a νMSM Sterile Neutrino.

Summary III and Conclusion

- Using data from Walker et. al. [3], we found a relationship between Q and r_{hf} of Milky Way dwarf satellite galaxies.

- We separated the dwarf galaxies into low and high σ groups, which enabled us to find the primordial radial scale r_p and the corresponding empirical Z factors for each group.

- With these Z factors, we were able to calculate Q_p and determine the mass of the dark matter particle for several theoretical models, including thermal relics [1] and sterile neutrinos [5].

Sources

- [1] Hogan, C. J. & Dalcanton, J. J. 2000, arXiv:astro-ph/0002330
- [2] de Vega, H. J. & Sanchez, N. G. 2010, arXiv: 0901.0922
- [3] Walker, M.G., Mateo, M., Olszewski, E. W., Peñarrubia, J., Evans, N. W., & Gilmore, G. 2009, arXiv:0906.0341
- [4] Song, H. & Lee, J. 2009, arXiv:0903.5095
- [5] Viel, M., Lesgourgues, J., Haehnelt, M. G., Matarrese, S., & Riotto, A. 2005, arXiv:astro-ph/0501562
- [6] Watson, C., Li, Z., & Polley, N., 2012, arXiv:1111.4217

Issues with Current Detectors II

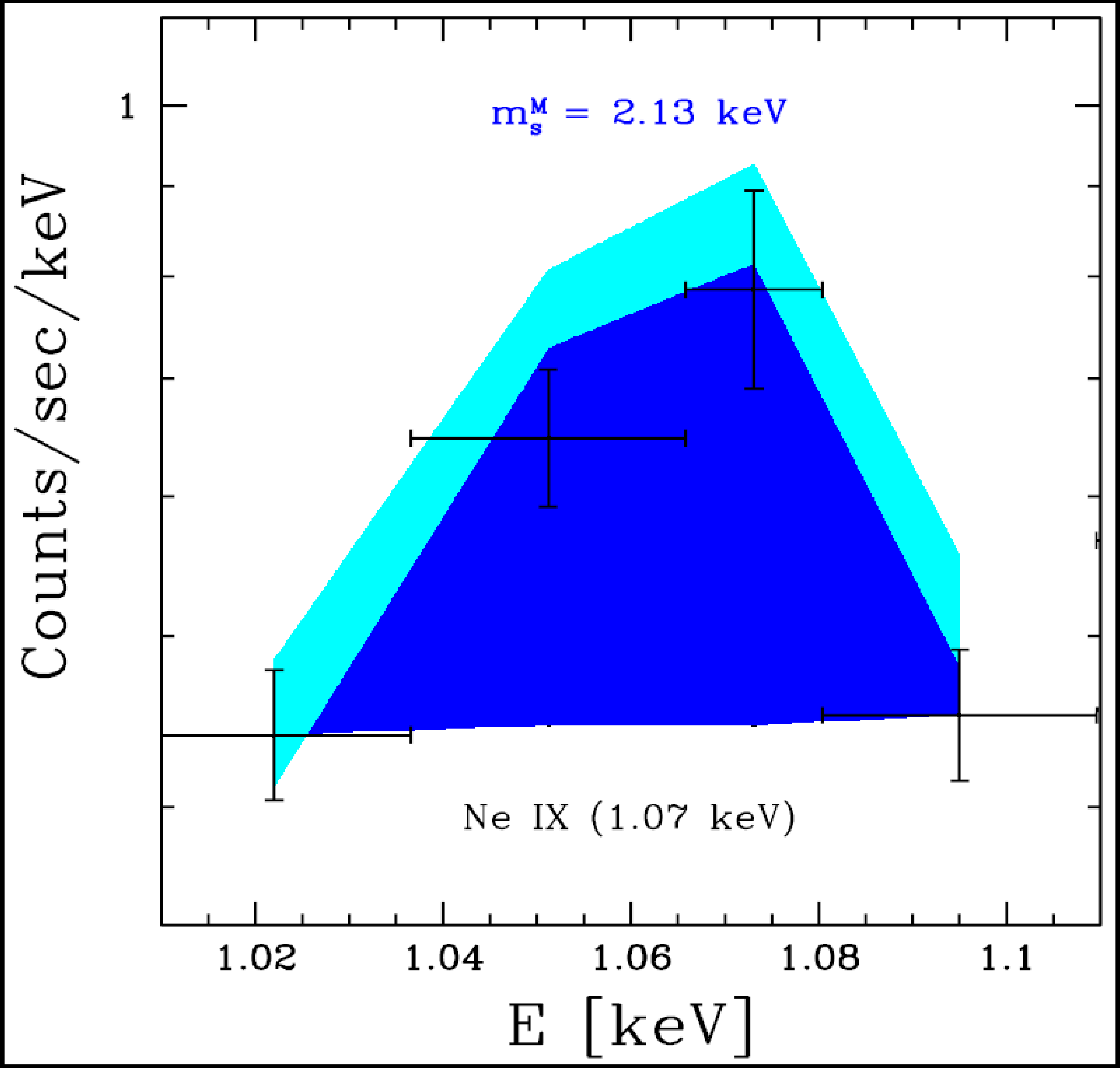

Based on Σ_{DM}^{FOV}

2.13 keV Majorana sterile neutrino decay statistically reproduces 1.07 keV Ne IX peak (Chandra Data).

Current Targets of Opportunity:

Dark Matter Filaments between Merging Galaxies

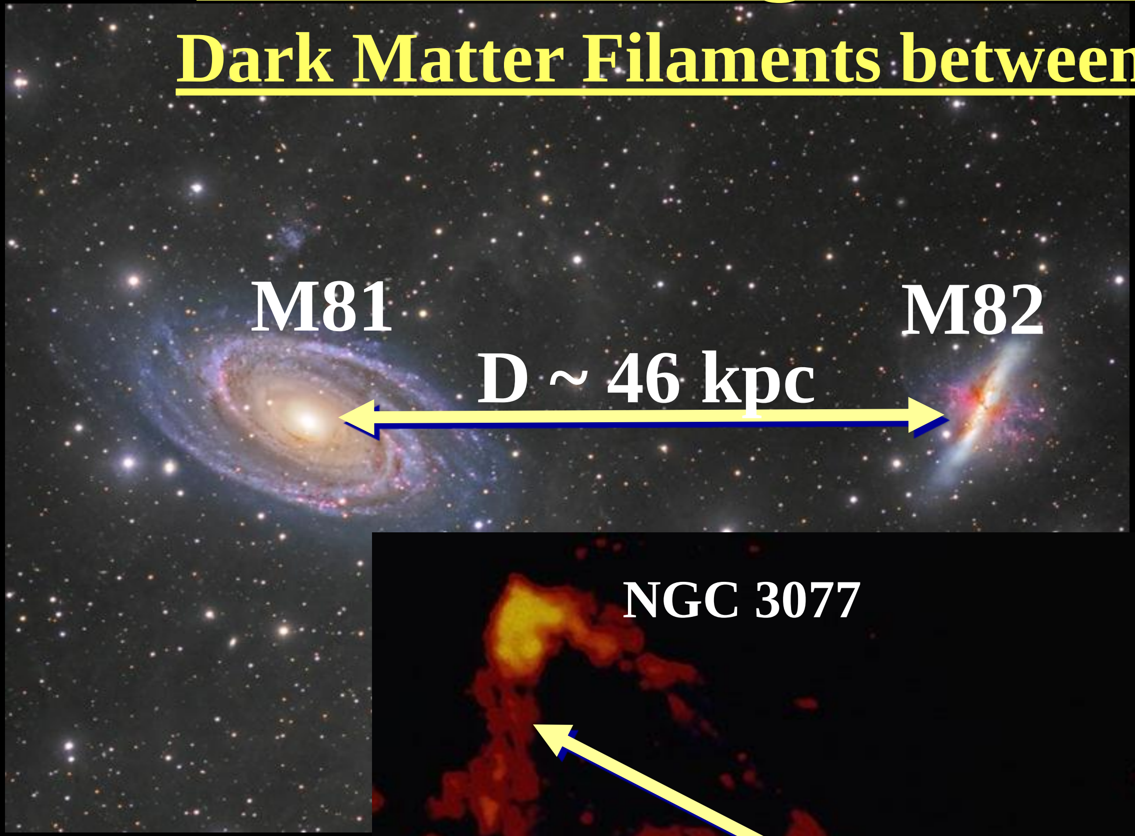

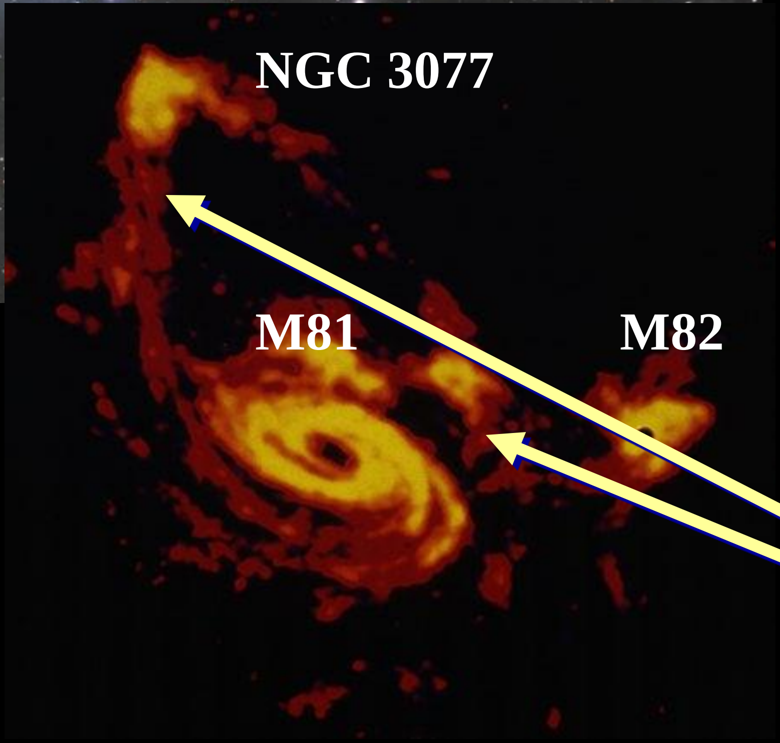

M81/M82 System

Excellent Laboratory for Examining DM Filaments

- **Nearby (3.6 Mpc)**
- **Small Separation**
- **Starburst Activity shows evidence of close pass 0.2-0.3 Gyrs**
  de Mello et al. (2007)
- **Radio Observations Reveal Extensive Network of Neutral Hydrogen Filaments**
  Chynoweth et al. (2008)

Simulated Dynamics & Filament Formation II:

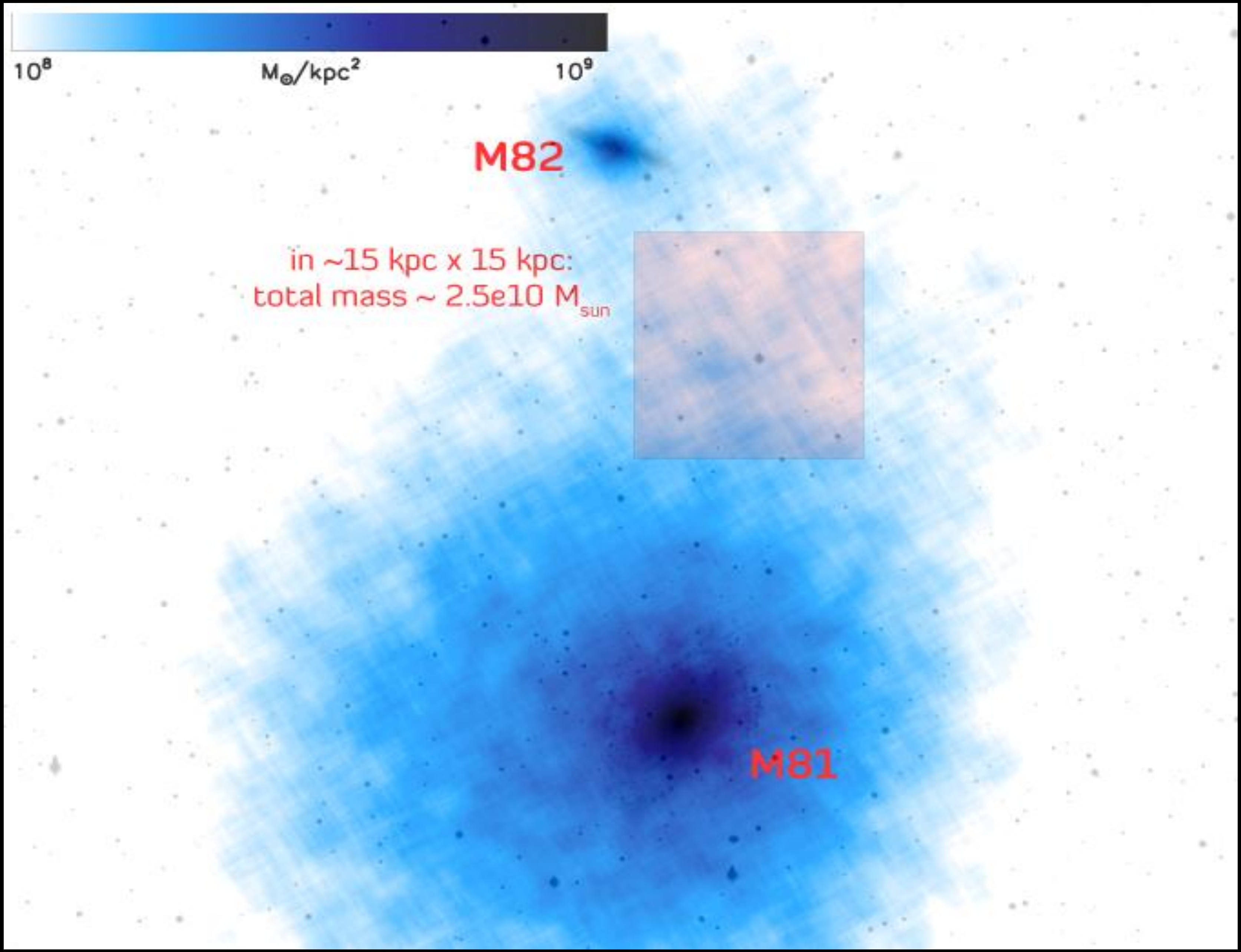

Proposed *Chandra* Observations:

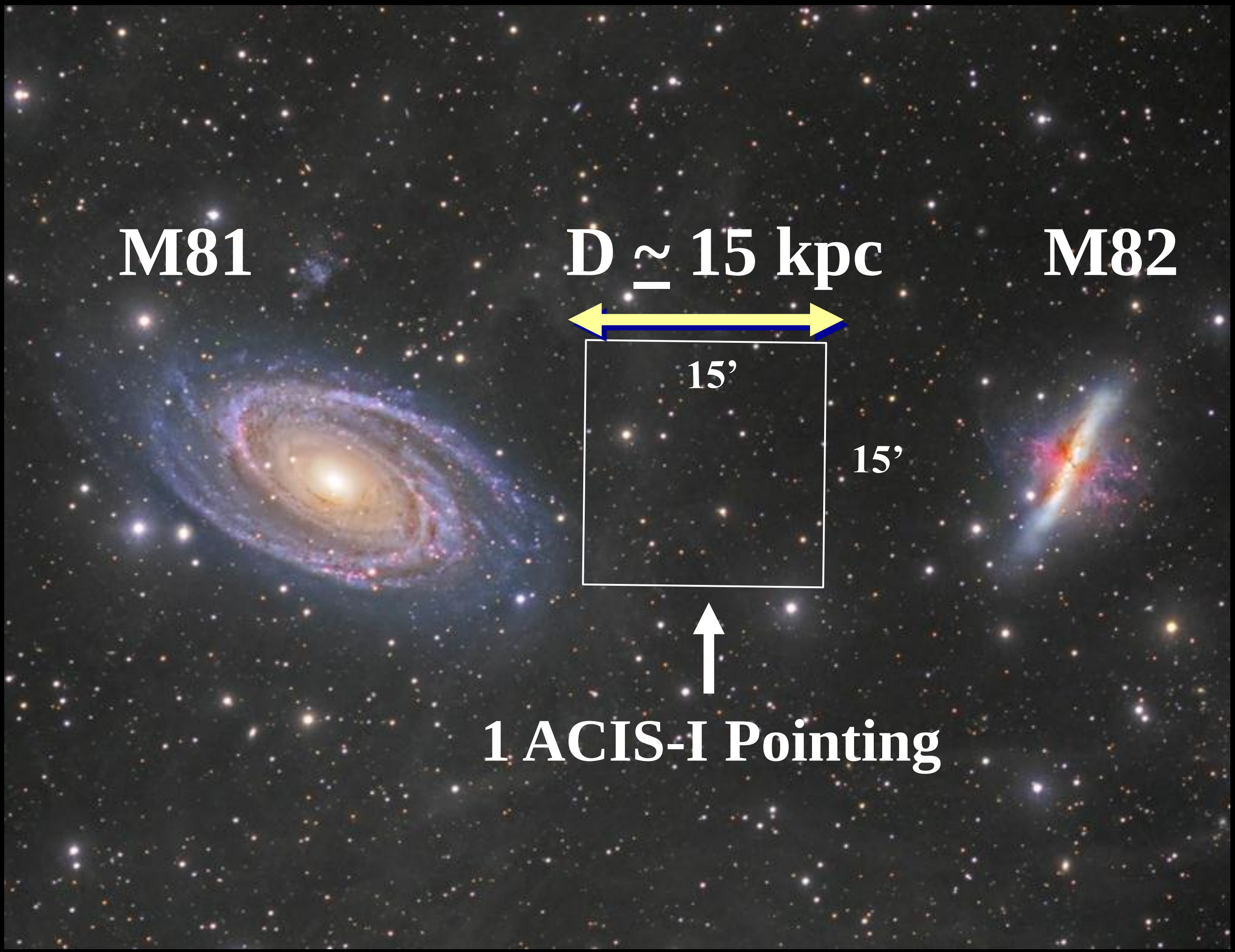

At D ~ 3.6 Mpc,
1' ~ 1 kpc

so

Only 1 *Chandra* ACIS-I Pointing needed to cover the space between M81 & M82 that should be relatively free of hot gas.

Forecast for Observations & Constraints:

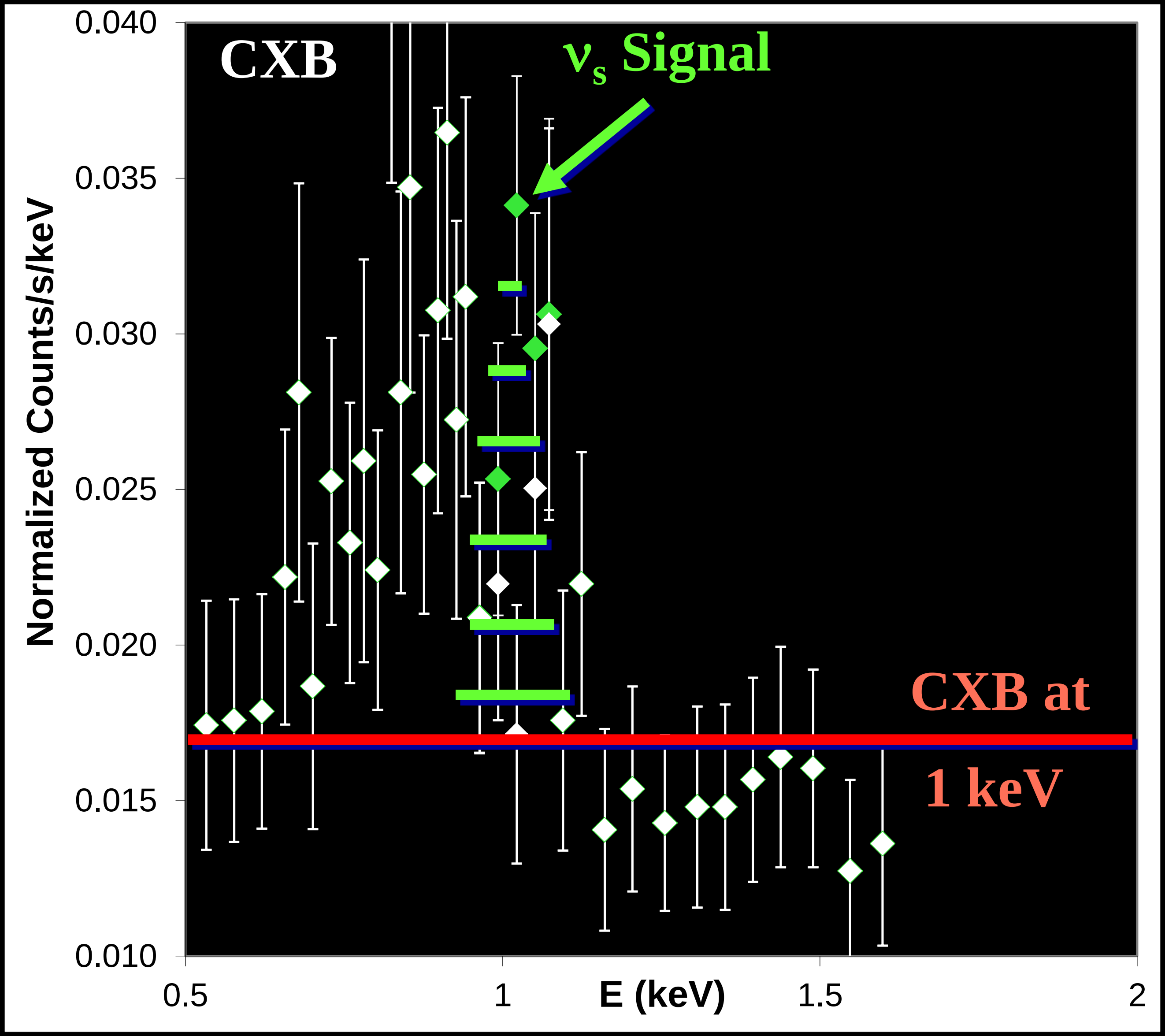

Prospective Data:
Chandra **CXB in**
a 15' x 15' FoV

M_{Fil} in FoV:
$2.5 \times 10^{10}\ M_\odot$

Σ_{FoV} ($10^{11} M_\odot Mpc^{-2}$)
$\Sigma_{fil} \simeq 0.019$
$\Sigma_{MW} \simeq 0.009$
(Low mass MW [76])
$\Sigma_{tot} \simeq 0.028$

ν_s Signal:
Exclusion/Detection
at m_s = 2 keV

Kinematic Evidence of Tidally Stripped Mass?

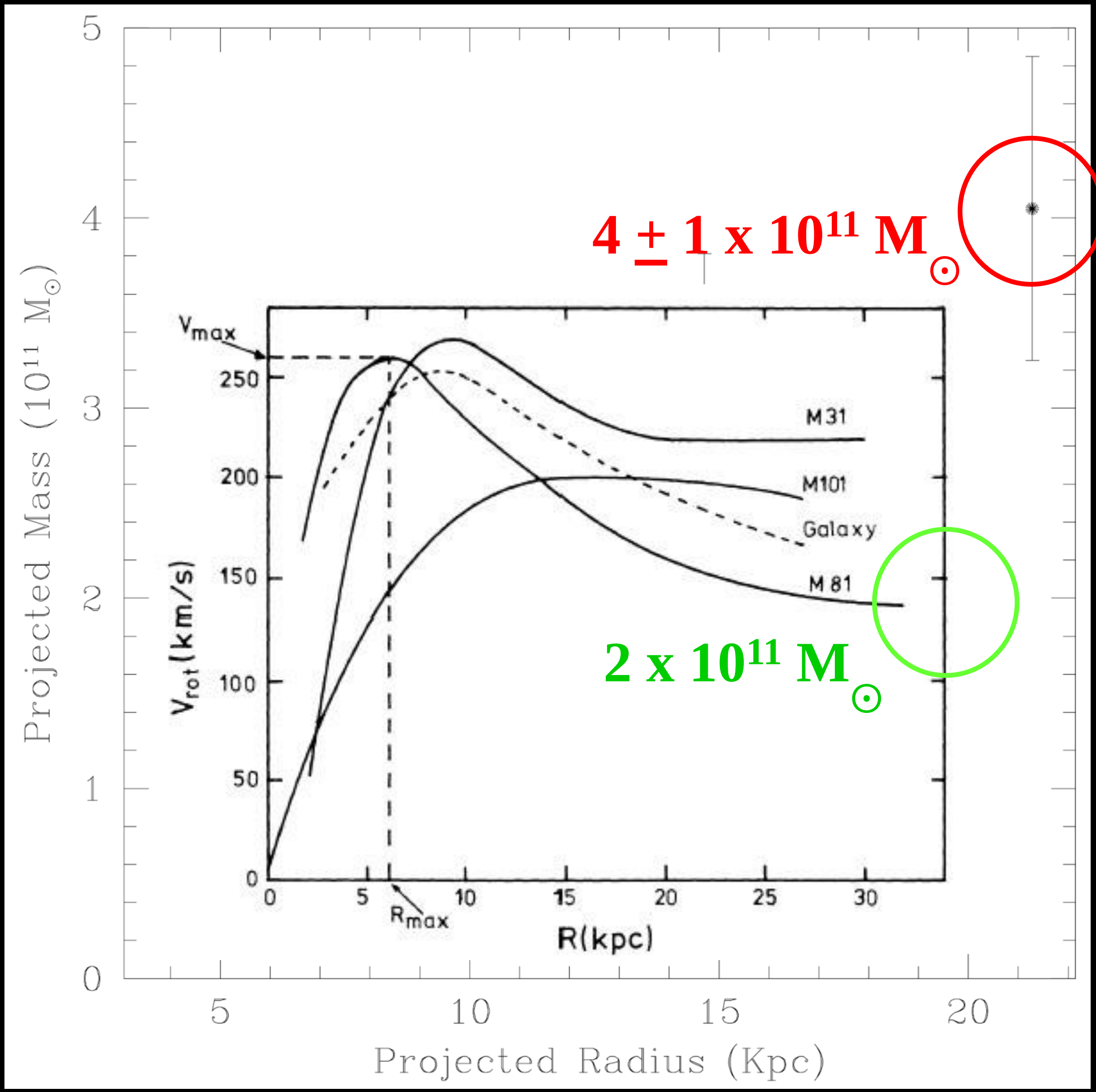

M81/M82 Group Mass:

~10^{12} $M_\odot$

Karachentsev & Kashibadze (2006)

M81 Mass:

~ 2 - 5 x 10^{11} $M_\odot$

Roberts & Rots (1973)

Schroder et al. (2001)

M82 Mass:

~ 10^{10} M

Greco et al. (2012)

Only 2 more "large" galaxies in group (both smaller than M81)

Mass Discrepancy points to possibility of significant filament(s).

Simulated Dynamics & Filament Formation I:

by Chris Purcell (Univ. of Pittsburgh: PITT PACC)

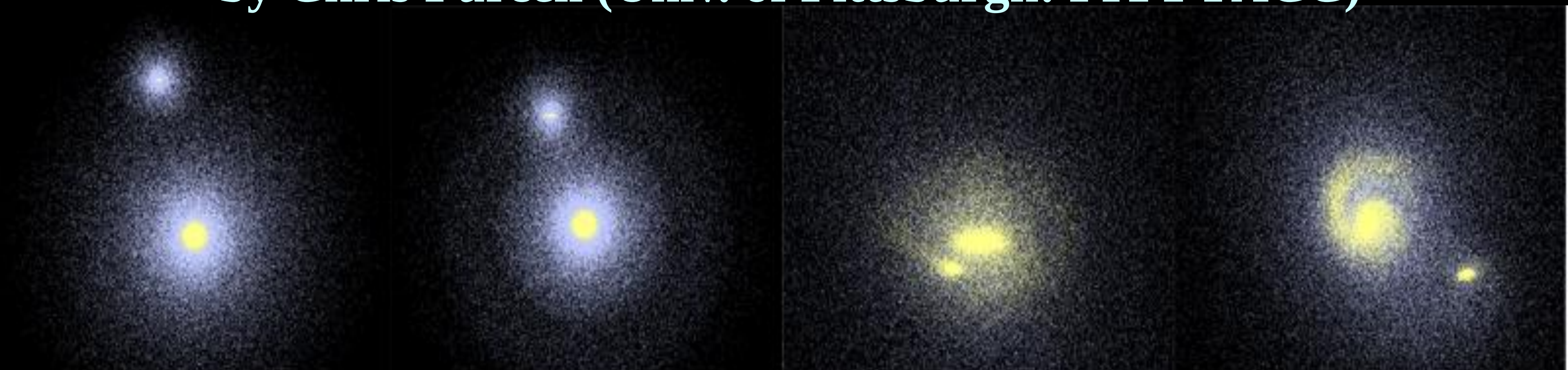

Initial Conditions:

M81 = $7\mathrm{x}10^{11}\ M_\odot$ (within 200 kpc)

M82 = $1\mathrm{x}10^{11}\ M_\odot$ (within 100 kpc)

$D_{separation}$ = 200 kpc

Infall vel. = 100 km/s

Sofue (1998)

Approach:

τ = 0.47 Gyrs

120 kpc

Pericenter:

τ = 0.89 Gyrs

16 kpc

Final State:

τ = 1.14 Gyrs

$\Delta\tau \sim$ 0.25 Gyr since pericenter

as in de Mello et al. (2007)

M81 $\simeq 5\mathrm{x}10^{11}\ M_\odot$

as in Schroder et al. (2001)

M82 = $10^{10}\ M_\odot$

as in Greco et al. (2012)

36 kpc